NATIONAL AERONAUTICS AND SPACE ADMINISTRATION

Technical Memorandum 33-687

Viscous, Radiating Hypersonic Flow About a Blunt Body

Richard S. Passamaneck

JET PROPULSION LABORATORY
CALIFORNIA INSTITUTE OF TECHNOLOGY
PASADENA, CALIFORNIA

May 1, 1974

Prepared Under Contract No. NAS 7-100
National Aeronautics and Space Administration

PREFACE

The work described in this report was performed by the Applied Mechanics Division of the Jet Propulsion Laboratory.

CONTENTS

TABLES

FIGURES

ABSTRACT

The viscous, radiating hypersonic flow past an axisymmetric blunt body is analyzed based on the Navier-Stokes equations, plus a radiative equation of transfer derived from the Milne-Eddington differential approximation. The fluid is assumed to be a perfect gas with constant specific heats, a constant Prandtl number, P, of order unity, a viscosity coefficient varying as a power, ω, of the temperature, and an absorption coefficient varying as the first power of the density and as a power, n, of the temperature.

The gray gas assumption is invoked, thereby making the absorption coefficient independent of the spectral frequency. Limiting forms of the solutions are studied as the freestream Mach number, M, freestream Reynolds number, R, and the temperature ratio across the shock wave, $\Gamma = \epsilon M^2$, go to infinity, and as the Bouguer number, Bu, and the density ratio across the shock wave, $\epsilon = (\gamma-1)/(\gamma+1)$, go to zero.

The method of matched asymptotic expansions is used in the analysis, and it is shown that there is a far-field precursor, composed of two regions, in which the fluid mechanics can be neglected for all practical purposes but are included for completeness. Also found is a near-field precursor in which the temperature rises to its shock structure order of magnitude. The high temperature in this region,

due to radiation transfer, causes the next region, the outer region of the shock structure, to be thicker by $O(\Gamma^{\omega})$ than the outer region without radiation. Next follows the middle and inner regions of the shock structure, with solutions differing only in the constants of integration from those found for the non-radiative problem. A radiation relaxation region between the shock structure and shock layer is now needed in order that radiative equilibrium can be obtained. The shock layer is unchanged from the non-radiative problem, except for the addition of $I = T^4$, and has two or three regions, depending on the ratios of the viscous to inviscid terms.

Chapter I

INTRODUCTION

The purpose of this paper is to isolate the important parameters of a viscous, radiating hypersonic flow past a blunt body of arbitrary shape. Much confusion and discussion have existed as to the importance of the radiative term's contribution to the energy equation in the various flow regions from the precursor field immediately ahead of the shock wave to the body surface, i.e., references [13] and [17].

In order to isolate the parameters, and the role they play, and to make the problem tractable, the gas is assumed to be perfect with an absorption coefficient that is independent of spectral frequency (the gray gas assumption). The gray gas assumption is a serious one in that spectral detail in the problem is completely omitted, which could allow the gas to range from a high absorption at one frequency to a low absorption at another frequency, thereby having absorption properties ranging from optically thick to optically thin in the same flow region. On the other hand, the gray gas assumption yields the problem analytically tractable, thereby allowing the functional behaviors of the various flow quantities from the freestream to the body to be found. If spectral detail were included, provided it were known, only numerical results could be hoped for, which would give no indication as to how the various flow quantities interact with each

other, Heaslet and Baldwin [11]. Figure 1 gives the results of Heaslet and Baldwin for the strong shock case. The parameter K/K' corresponds to the inverse of the Boltzmann number that is used in the present analysis.

Most analyses up to now have assumed that the various regions of flow were either optically thick (the Rosseland approximation) or optically thin (the Planck approximation), Emanuel [6], Jische [12], Burggraff [2], and Olfe [15]. The thick and thin approximations are the lower and upper limits, respectively, of the photon mean free path and therefore are even more restrictive than the gray gas assumption. These two approximations have the additional serious drawback that one of the two conditions for similarity is eliminated. More specifically, the thick and thin approximations identically satisfy the radiative transfer equation, thereby eliminating the Bouguer number, inverse characteristic optical length, and its importance as a similarity parameter. Although the Bouguer number appears in the energy equation it appears only in the ratio of Bouguer number to Boltzmann number. On the other hand, the condition for "full similarity" is the equivalence of the ratio Bu/Bo and the Bouguer number. In the present treatment, the full coupling of the fluid mechanics and radiative transfer are used, with the details of the analysis being the determining factor as to whether or not the set of equations are radiatively thick, coupled, or thin for a given flow region.

The problem treated here uses as its starting point the problem treated by Bush [3], with the exception that radiation is included in the equations of motion, so that changes in the flow quantities in the

various flow regions due to radiation, as well as the need for additional regions, must be considered. For this case the Boltzmann number (ratio of the convected energy to the radiated black body energy at stagnation conditions), $Bo = (\rho_\infty U_\infty C_{p_1} T_o)/\sigma T_o^4$, is of order one, the freestream Mach number, $M = U_\infty/(\gamma p_\infty/\rho_\infty)^{\frac{1}{2}}$, and the Reynolds number, $R = (\rho_\infty U_\infty a)/\mu_\infty$, go to infinity, and the density ratio, $\epsilon = (\gamma-1)/(\gamma+1)$, the Bouguer number, $Bu = \alpha_\infty a$, and $Q = Bu\Gamma^{n+\omega}/\epsilon R$ (ratio of the molecular mean free path to the photon mean free path at shock layer conditions), go to zero.

Since, consistent with the radiating hypersonic blunt body problem, the freestream Bouguer number is very very small, it is required that a precursor field ahead of the body have a large scale thickness of the order $Bu^{-1} = 10^{10}$ body radii, Nelson and Goulard [14]. This extremely large region precludes any chance of applying a thin layer analysis to it. (A region such as this is physically consistent with the fact that an observer at a large distance from the body can "see" a body under these conditions due to the photons emitted from the shock layer of the body.) It should also be noted that this "far-field precursor" is two-dimensional in nature and the equations are those of the field type. This is true because the addition of the equation of radiative transfer makes the entire set of equations of motion elliptic rather than hyperbolic, which is normally true for the region ahead of the shock in hypersonic flow. In view of this extreme analytical difficulty, the far-field precursor will simply be assumed to be one-dimensional in which an exponent approximation is

valid. Thus the far-field precursor is found to have two regions which are designated as the exterior and the interior regions.

As the flow approaches the body, more photons are absorbed by the gas and consequently the temperature, pressure and intensity increase. In the case under consideration, the gas temperature rises to the shock layer order of magnitude, although still smaller by a constant multiple less than one, Heaslet and Baldwin [11]. With this relatively high temperature, the gas is capable of absorbing and emitting in a thin region ahead of the shock structure. This region is referred to as the "near-field precursor" and is the first thin region in the flow field, and thus the first that can be considered without using a one-dimensional approximation. This region has a scale thickness of order $(1/Bu\Gamma^{n})\ll 1$ with the velocity components and density having only correction terms. Figure 2 gives the schematic for the flow region.

The optically thin outer region of the shock structure, with thickness $O(1/R)$, is expected to be the next region, but the increased temperature causes this layer to be thicker by Γ^{ω} and consequently the corrections on the velocity components and density are different from the corrections for the conventional outer region. Since this region is now of the same scale thickness as the middle region, $O(\Gamma^{\omega}/R)\ll 1$, it is expected that they would have a different effective thickness. In the analysis it is shown that the middle region has an effective thickness equal to $O(\Gamma^{\omega}/R)\log R/Bu\Gamma^{n+\omega}$. It should be noted that the outer region does not "see" freestream

infinity when looking upstream and thus the boundary conditions for the fluid mechanical shock are not found in the conventional way. Now the precursor-induced conditions, due to the upstream heating of the gas, are the conditions to which the fluid mechanical shock must be matched.

The middle region of the shock structure is the next region of flow after the outer region. The scalings and solutions are the same as those found by Bush [3] with the exception that a constant of integration appears in the temperature and pressure solutions. The equation of radiative transfer shows that this region, which has a scale thickness of $O(\Gamma^{\omega}/R)$, is optically thin, Vincenti and Kruger [21]. (Since the inner region of the shock structure has a scale thickness equal to $O(\epsilon\Gamma^{\omega}/R)$, it will also be optically thin.) Since this middle region is optically thin, the intensity is scaled as a correction to the value it has previously obtained.

The next region after the middle region is the inner region, as found by Bush [3]. The scalings, thickness and solutions of the region are the same as for the nonradiating problem. The intensity is still scaled as a constant plus a correction. Since the inner region is thin in order of magnitude, it "sees" an infinity when looking downstream, and therefore the fluid mechanical shock conditions, consistent with the flow conditions, are found as in the nonradiating case. In the strict mathematical sense, the inner region does not match to the radiation relaxation region, which is the next region in this analysis. In order to match these two regions, higher order terms must be included and the reader is referred to Bush [4] for the matching.

Between the shock structure and the shock layer a new region is present. This region is referred to as the radiation relaxation region and is one which allows the intensity to equilibrate with its equilibrium conditions, Heaslet and Baldwin [11]. The fluid mechanics of this region are minimal. The scale thickness of this region is $O(\epsilon/Bu\Gamma^{n})$, which is much larger than the middle region thickness, $O(\Gamma^{\omega}/R)$. This is a result of the fact that the photon mean free path is much larger than the molecular mean free path as shown by Bond, Watson and Welch [1] and Zel dovich and Raiser [22]. Also since $Bu\Gamma^{n} \gg O(1)$, the following ordering sequence occurs: $\Gamma^{\omega}/R \ll \epsilon/Bu\Gamma^{n} \ll \epsilon$. Since $K = \Gamma^{\omega}/\epsilon R \to 0$ implies that the shock layer can only be inviscid, Bush [3], i.e., the possibility of the viscous shock layer, $K = O(1)$, is eliminated. The radiation relaxation region "sees" an infinity when looking toward the body, and therefore a second set of shock conditions due to the radiation effect are found. Thus the near-field precursor region and the radiation relaxation can be thought of as the radiation shock, with its appropriate boundary conditions, and the outer region, middle region and inner region of the shock structure can be thought of as the fluid mechanical shock, with its appropriate boundary conditions, imbedded within the radiation shock. This double shock is referred to as a shock within a shock by Vincenti and Kruger [21].

The shock layer follows the radiation relaxation region, and for the flow conditions it is optically thick and in radiative equilibrium with the surroundings. The scalings and order of magnitude thickness

are the same as found by Bush [3] and the shock layer has two or three distinct layers for the same reasons as in the nonradiating problem. Table 1 summarizes the shock layer. The only difference is the intensity as an independent variable.

TABLE 1

$K = \Gamma^{\omega}/\epsilon R \to 0$	$D = \Gamma^{\omega}/\epsilon^{5/2}R$
$D = O(1)$	inviscid shock layer + viscous body layer
$D \to 0$	inviscid shock layer + inviscid body layer + viscous boundary layer

To summarize: the exterior region of the far-field precursor has thickness of $O(1/Bu) \gg 1$ and the interior region of the far-field has scale thickness of $O(1/Bu)$ and an effective thickness of $O(1/Bu)\log \Gamma^3 \gg O(1/Bu)$. The near-field precursor has a thickness of $O(1/Bu\Gamma^n) \ll 1$ and the outer region of the shock structure has a thickness of $O(\Gamma^{\omega}/R) \ll O(1/Bu\Gamma^n)$. The middle region is $O(\Gamma^{\omega}/R)$ in scale thickness but has an effective thickness of $O(\Gamma^{\omega}/R)\log(R/Bu\Gamma^{n+\omega}) \gg O(\Gamma^{\omega}/R)$. It is also true that $O(\Gamma^{\omega}/R)\log(R/Bu\Gamma^{n+\omega}) \ll O(1/Bu\Gamma^n)$. For the inner region the thickness is $O(\epsilon\Gamma^{\omega}/R) \ll O(\Gamma^{\omega}/R)$ since $\epsilon \to 0$. In the relaxation region the thickness is $O(1/Bu\Gamma^n) \gg O(\Gamma^{\omega}/R)$.

Chapter II

THE EQUATIONS OF MOTION

Consider the hypersonic flow of a viscous, radiating gas past an axially symmetric blunt body. An orthogonal curvilinear coordinate system, with the body surface as reference, is used. Let $x_1 = ax$ and $y_1 = ay$, respectively, represent the distance measured along the body from the stagnation point and the distance measured normal to the body at the corresponding x_1 location. The length, a, is the nose radius of the body, Figure 3.

With the above non-dimensionalization, the curvature of the body surface and the body meridian radius become, respectively, $\kappa_1 = \kappa/a$ and $B_1 = aB$. The velocity components in the x_1 and y_1 directions, respectively, are $u_1 = U_\infty u$ and $v_1 = U_\infty v$ and the pressure, density, temperature, and intensity, respectively, are $p_1 = p_\infty p$, $\rho_1 = \rho_\infty \rho$, $T_1 = T_\infty T$, and $I_1 = \sigma T_o^4 I$. The quantities U_∞, p_∞, ρ_∞, T_∞, and σT_o^4, respectively, are the freestream velocity, pressure, density, temperature, and the black body radiation present in the stagnation region.

A perfect gas is assumed ($p = \rho T$) having constant specific heats (C_{v_1}, C_{p_1}, and $\gamma = C_{p_1}/C_{v_1} = \text{const.}$). The Prandtl number is assumed to be of order one, $P = O(1)$, with the viscosity coefficient being proportional to the power, ω, of the absolute temperature, ($\mu_1 = \mu_\infty \mu = \mu_\infty T^\omega$), where $\frac{1}{2} \leq \omega \leq 3/2$. The radiative absorption coefficient is assumed to be independent of spectral frequency (the gray

gas assumption) and proportional to the first power of the density and the power, n, of the temperature ($\alpha_1 = \alpha_\infty \alpha = \alpha_\infty \rho T^n$). For molecular radiation of a monotonic gas, n = 6, Thomas [18], Goulard [9], and Penner and Olfe [16].

The Navier-Stokes equations are assumed to be valid. The radiative pressure terms in the momentum and energy equations have been neglected, since they are negligible in all regions of flow considered, Goulard [8]. The addition of the radiative term to the energy equation is therefore the only change that is necessary to the continuity, momentum and energy equations that are valid for nonradiating flows. An additional variable, the intensity, requires the inclusion of a radiative equation of transfer. This is accomplished by using the Milne-Eddington differential approximation:

$$\frac{1}{h}\left(\frac{\partial q_{x_1}}{\partial x_1} + \frac{\partial q_{y_1}}{\partial y_1} + \frac{\kappa_1 q_{y_1}}{r_1}\right) + \left(\frac{q_{x_1} \sin\varphi + q_{y_1} \cos\varphi}{r_1}\right)$$

$$= -\alpha_1 \left(I_1 - 4\sigma T_1^4\right),$$

$$\frac{1}{h}\frac{\partial I_1}{\partial x_1} = -3\alpha_1 q_{x_1},$$

$$\frac{\partial I_1}{\partial y_1} = -3\alpha_1 q_{y_1}.$$

The components of the radiative heat flux vector are eliminated by differentiation in favor of the integrated intensity, thus yielding:

$$\frac{1}{h}\left(\frac{\partial}{\partial x_1}\left[\frac{1}{h\alpha_1}\frac{\partial I_1}{\partial x_1}\right]+\frac{\partial}{\partial y_1}\left[\frac{1}{\alpha_1}\frac{\partial I_1}{\partial y_1}\right]+\frac{\kappa_1}{\alpha_1 r_1}\frac{\partial I_1}{\partial y_1}\right)$$

$$+\frac{1}{\alpha_1 r_1}\left(\frac{1}{h}\frac{\partial I_1}{\partial x_1}\sin\varphi+\frac{\partial I_1}{\partial y_1}\cos\varphi\right)=3\alpha_1\left(I_1-4\sigma T_1^4\right).$$

Traugott, [19] and [20], performed a shock structure analysis by eliminating the intensity in favor of the heat flux vector, which had been assumed to be one-dimensional. The equations of motion under the above conditions are:

$$\frac{\partial(\rho v)}{\partial y}+\frac{1}{h}\frac{\partial(\rho u)}{\partial x}+\frac{\kappa\rho v}{h}+\frac{\rho(u\sin\varphi+v\cos\varphi)}{r}=0\,, \tag{2.1}$$

$$\begin{aligned}&\rho\left(\frac{u}{h}\frac{\partial u}{\partial x}+v\frac{\partial u}{\partial y}+\frac{\kappa uv}{h}\right)+\frac{1-\epsilon}{1+\epsilon}\frac{1}{M^2}\frac{1}{h}\frac{\partial p}{\partial x}\\&\quad=\frac{1}{R}\left[\left(\frac{\partial}{\partial y}+\frac{2\kappa}{h}+\frac{\cos\varphi}{r}\right)\left(\mu\left[\frac{\partial u}{\partial y}-\frac{\kappa u}{h}+\frac{1}{h}\frac{\partial v}{\partial x}\right]\right)\right.\\&\quad+\frac{2}{3}\frac{1}{h}\frac{\partial}{\partial x}\left(\mu\left[\frac{2}{h}\left\{\frac{\partial u}{\partial x}+\kappa v\right\}-\frac{\partial v}{\partial y}-\frac{u\sin\varphi+v\cos\varphi}{r}\right]\right)\\&\quad\left.+\frac{2\sin\varphi}{r}\left(\mu\left[\frac{1}{h}\left\{\frac{\partial u}{\partial x}+\kappa v\right\}-\frac{u\sin\varphi+v\cos\varphi}{r}\right]\right)\right]\,,\end{aligned} \tag{2.2}$$

$$\begin{aligned}&\rho\left(\frac{u}{h}\frac{\partial v}{\partial x}+v\frac{\partial v}{\partial y}-\frac{\kappa u^2}{h}\right)+\frac{1-\epsilon}{1+\epsilon}\frac{1}{M^2}\frac{\partial p}{\partial y}\\&\quad=\frac{1}{R}\left[\left(\frac{4}{3}\frac{\partial}{\partial y}+\frac{2\kappa}{h}+\frac{2\cos\varphi}{r}\right)\left(\mu\frac{\partial v}{\partial y}\right)\right.\end{aligned}$$

$$+\left(\frac{1}{h}\frac{\partial}{\partial x}+\frac{\sin\varphi}{r}\right)\left(\mu\left[\frac{\partial u}{\partial y}-\frac{\kappa u}{h}+\frac{1}{h}\frac{\partial v}{\partial x}\right]\right) \tag{2.3}$$

$$-\left(\frac{2}{3}\frac{\partial}{\partial y}+\frac{2\kappa}{h}\right)\left(\mu\left[\frac{1}{h}\left\{\frac{\partial u}{\partial x}+\kappa v\right\}\right]\right)$$

$$-\left(\frac{2}{3}\frac{\partial}{\partial y}+\frac{2\cos\varphi}{r}\right)\left(\mu\,\frac{u\sin\varphi+v\cos\varphi}{r}\right)\Bigg],$$

$$\rho\left(\frac{u}{h}\frac{\partial T}{\partial x}+v\frac{\partial T}{\partial y}\right)-\frac{2\epsilon}{1+\epsilon}\left(\frac{u}{h}\frac{\partial p}{\partial x}+v\frac{\partial p}{\partial y}\right)=\frac{1}{PR}\Bigg[\frac{\partial}{\partial y}\left(\mu\frac{\partial T}{\partial y}\right)$$

$$+\left(\frac{\kappa}{h}+\frac{\cos\varphi}{r}\right)\mu\frac{\partial T}{\partial y}+\frac{1}{h}\frac{\partial}{\partial x}\left(\frac{\mu}{h}\frac{\partial T}{\partial x}+\frac{\sin\varphi}{r}\frac{\mu}{h}\frac{\partial T}{\partial x}\right)\Bigg] \tag{2.4}$$

$$+\frac{2\epsilon M^2}{1-\epsilon}\frac{\mu}{R}\Bigg[2\left(\frac{\partial v}{\partial y}\right)^2+2\left(\frac{1}{h}\left\{\frac{\partial u}{\partial x}+\kappa v\right\}\right)^2+2\left(\frac{u\sin\varphi+v\cos\varphi}{r}\right)^2$$

$$+\left(\frac{\partial u}{\partial y}-\frac{\kappa u}{h}+\frac{1}{h}\frac{\partial v}{\partial x}\right)^2-\frac{2}{3}\left(\frac{1}{h}\frac{\partial h}{\partial x}+\frac{\partial v}{\partial y}+\frac{\kappa v}{h}\right.$$

$$\left.+\frac{u\sin\varphi+v\cos\varphi}{r}\right)^2\Bigg]+\frac{\alpha Bu}{B_o}\Gamma\left(I-4\Gamma^{-4}T^4\right),$$

$$\frac{1}{h}\left(\frac{\partial}{\partial x}\left[\frac{1}{h}\frac{1}{\alpha}\frac{\partial I}{\partial x}\right]+\frac{\partial}{\partial y}\left[\frac{1}{\alpha}\frac{\partial I}{\partial y}\right]+\frac{\kappa}{r}\frac{1}{\alpha}\frac{\partial I}{\partial y}\right)$$

$$+\frac{1}{r}\frac{1}{\alpha}\left(\frac{1}{h}\frac{\partial I}{\partial x}\sin\varphi+\frac{\partial I}{\partial y}\cos\varphi\right)=3\alpha Bu^2\left(I-4\Gamma^{-4}T^4\right), \tag{2.5}$$

$$p=\rho T\,, \tag{2.6}$$

$$\mu=T^{\omega}\,, \tag{2.7}$$

$$\alpha=\rho T^{n}, \tag{2.8}$$

where $h = 1 + \kappa(Y + y)$, $r = B + (Y + y)\cos\varphi$, $\epsilon = \gamma-1/\gamma+1 \to 0$ (the Newtonian approximation), $M^2 = \rho_\infty U_\infty{}^2/\gamma p_\infty \gg 1$, $R = \rho_\infty U_\infty a/\mu_\infty \gg 1$, the Boltzmann number, $Bo = \rho_\infty U_\infty C_p T_o/\sigma T_o{}^4 = O(1)$, $\Gamma = T_o/T_\infty \gg 1$, and the characteristic optical length, $Bu^{-1} \gg 1$.

Along with the above equations of motion one additional equation, in the form of a boundary condition, must be satisfied in conjunction with equation (2.5). This equation is:

$$\left.\frac{\partial I}{\partial y}\right|_{lim} = \sqrt{3}\, Bu\, \alpha\, (I_{lim} - 4\Gamma^{-4} T_B{}^4) \tag{2.9}$$

where I_{lim} and $\left.\frac{\partial I}{\partial y}\right|_{lim}$ are taken in the limit as they approach the downstream boundary of the region, and T_B is the temperature at the upstream limit of the region immediately downstream. Equation (2.9) is implicitly satisfied at each boundary.

Chapter III

THE EXTERIOR REGION OF THE FAR-FIELD PRECURSOR

With a body in hypersonic flow, traveling sufficiently fast so as to induce electro-magnetic radiation, the flow quantities start deviating from their freestream values prior to their encounter with the "shock wave." The precursor effect is due to the generation of electro-magnetic radiation in the shock layer, which is propagated upstream at its characteristic speed of light.

The first region of the far-field precursor is the exterior region. The scale thickness of this region has an order of magnitude thickness, $(Bu)^{-1}$, equal to $O(10^{10})$ body radii. Although this region is two-dimensional, it will be assumed that it is one-dimensional in order that analytic solutions may be obtained. This assumption is valid since the changes in the flow quantities are small and therefore would not significantly affect regions that follow downstream. This region has the pressure and temperature varying as corrections to their freestream values. The corrections to the velocity components and density are very small but are included for completeness. The intensity is scaled from its freestream value. The coordinates and flow quantities consistent with the above description are:

$$y = \frac{1}{Bu}\, y_e; \tag{3.1}$$

$$u = \cos\varphi + \frac{\epsilon r^{-3}}{M^2}\, u_e + \cdots ,$$

$$v = -\sin\varphi + \frac{r^{-3}}{M^2}\, v_e + \cdots ,$$

$$p = 1 + \Gamma^{-3}\, p_e + \cdots \,, \tag{3.2}$$

$$\rho = 1 + \frac{\Gamma^{-3}}{M^2}\, \rho_e + \cdots \,,$$

$$T = 1 + \Gamma^{-3}\, T_e + \cdots \,,$$

$$I = 4\Gamma^{-4}\, I_e + \cdots \,.$$

Substitution of (3.1) and (3.2) into the equations of motion, (2.1)-(2.8), yields, to first order, the following:

$$\begin{gathered} p_e = T_e \,, \quad v_e - \rho_e \sin\varphi = 0 \,, \\ -\sin\varphi \frac{\partial v_e}{\partial y_e} + \frac{\partial p_e}{\partial y_e} = 0 \,, \quad -\sin\varphi \frac{\partial u_e}{\partial y_e} - Y_e' \frac{\partial p_e}{\partial y_e} = 0 \,, \\ -\sin\varphi \frac{\partial T_e}{\partial y_e} = \frac{4}{Bo} (I_e - 1) \,, \\ \frac{\partial^2 I_e}{\partial y_e^2} = 3 (I_e - 1) \,. \end{gathered} \tag{3.3}$$

The solutions to equations (3.3) are:

$$\begin{gathered} p_e = T_e = \frac{4J_e}{\sqrt{3}\, Bo \sin\varphi}\, e^{-\sqrt{3}\, y_e} \,, \quad \rho_e = \frac{1}{\sin^2\varphi}\, T_e \,, \\ v_e = \frac{1}{\sin\varphi}\, T_e \,, \quad u_e = -\frac{Y_e'}{\sin\varphi}\, T_e \,, \\ I_e = 1 + J_e\, e^{-\sqrt{3}\, y_e} \,, \end{gathered} \tag{3.4}$$

where it should be noted, due to the one-dimensional assumption, that J_e is not a function of x.

Chapter IV

THE INTERIOR REGION OF THE FAR-FIELD PRECURSOR

The next region is the interior region of the far-field precursor. In this interior region, the intensity is much larger than its free-stream order of magnitude, but still small compared to the stagnation order of magnitude it attains downstream. The pressure and temperature are still of their freestream order of magnitude and are scaled correspondingly. The velocity components and density are again scaled as the fluid mechanical aspects of this region are still small. The scale thickness of this interior region is the same as that of the exterior region; i.e., $O(Bu^{-1})$, but has an effective thickness order of magnitude which is much larger. Hence the coordinates and flow quantities have the following representations:

$$y = \frac{1}{Bu}\, y_j \ ; \tag{4.1}$$

$$u = \cos\varphi + \frac{\epsilon}{M^2}\, u_j + \cdots \ ,$$

$$v = -\sin\varphi + \frac{1}{M^2}\, v_j + \cdots \ ,$$

$$p + p_j + \cdots \ , \tag{4.2}$$

$$\rho = 1 + \frac{1}{M^2}\rho_j + \text{---} \ ,$$

$$T = T_j + \text{---} \ ,$$

$$I = 4\Gamma^{-1} I_j + \text{---} \ .$$

Substitutions of (4.1) and (4.2) into the equations of motion (2.1)-(2.8), yields, to the leading order, the following:

$$\begin{aligned}
&p_j = T_j \ , \quad v_j - \rho_j \sin\varphi = 0 \ , \\
&-\sin\varphi \frac{\partial v_j}{\partial y_j} + \frac{\partial p_j}{\partial y_j} = 0 \ , \quad -\sin\varphi \frac{\partial u_j}{\partial y_j} - Y_j' \frac{\partial p_j}{\partial y_j} = 0 \ , \\
&-\sin\varphi \frac{\partial T_j}{\partial y_j} = \frac{4}{Bo} T_j^{\,n} I_j \ , \\
&\frac{\partial}{\partial y_j}\left(\frac{1}{T_j^{\,n}} \frac{\partial I_j}{\partial y_j}\right) = 3 T_j^{\,n} I_j \ .
\end{aligned} \tag{4.3}$$

The solutions are most conveniently found by transforming the independent variables from y_j to T_j. Hence the solutions, in terms of T_j, are:

$$\begin{aligned}
p_j &= T_j \ , \\
\rho_j &= \frac{1}{\sin^2\varphi} T_j \ , \\
v_j &= \frac{1}{\sin\varphi} T_j \ ,
\end{aligned} \tag{4.4}$$

$$u_j = - \frac{Y'_j}{\sin\varphi} T_j \quad ,$$

$$I_j = \frac{\sqrt{3}\ Bo\ \sin\varphi}{4} (T_j - 1) \quad ,$$

$$y_j = - \frac{1}{\sqrt{3}} \int_{A_j}^{T_j} \frac{1}{\tau^n (\tau - 1)} d\tau \quad ,$$

where, for convenience, $A_j = 1 + \dfrac{4J_j}{\sqrt{3}\ Bo\ \sin\varphi}$.

The solutions in the limit as $y_j \to \infty$ are:

$$p_j = T_j = 1 + \frac{4J_j}{\sqrt{3}\ Bo\ \sin\varphi} e^{-\sqrt{3}\ y_j} \quad ,$$

$$\rho_j = \frac{1}{\sin^2\varphi} T_j \quad ,$$

$$v_j = \frac{1}{\sin\varphi} T_j \quad , \qquad (4.5)$$

$$u_j = - \frac{Y'_j}{\sin\varphi} T_j \quad ,$$

$$I_j = J_j\ e^{-\sqrt{3}\ y_j} \quad ,$$

and in the limit as $y_j \to 0$:

$$p_j = T_j = \frac{1}{(\sqrt{3}\ n\ y_j)^{1/n}} \quad ,$$

$$v_j = \frac{1}{\sin\varphi} T_j \quad , \qquad (4.6)$$

$$\rho_j = \frac{1}{\sin^2\varphi} T_j \quad ,$$

$$u_j = - \frac{Y'_j}{\sin\varphi} T_j \quad ,$$

$$I_j = \frac{\sqrt{3}\, Bo \sin\varphi}{4} \frac{1}{(\sqrt{3}\, n\, y_j)^{1/n}} \quad .$$

The matching of the interior region of the far-field precursor to the exterior region of the far-field precursor is accomplished using the normal coordinate as the matching variable, i.e., $\vec{\vec{y}}_1 = (K_j Z_j - y)/\vec{\vec{\lambda}}_1$ where $Bu\, \vec{\vec{\lambda}}_1 \to \infty$. Through the matching, it is found that $J_j = J_e$ (not functions of x), $K_j = 1/\sqrt{3}$ and the effective thickness, $Z_j = (1/Bu) \log \Gamma^3$.

Chapter V

THE NEAR-FIELD PRECURSOR REGION

In the near-field precursor region, the intensity and temperature rise to their shock layer orders of magnitude, whereas the pressure has risen to the order of magnitude it has in the middle region of the shock structure. The thickness of this region, $O(1/Bu\Gamma^n)$, is much less than one, but is much larger than the order of magnitude thickness of the shock structure. The velocity components and density vary as corrections to their freestream values. Hence, the coordinates and flow quantities have the following representations:

$$x = x_r \ , \quad y = \epsilon Y_r(x_r) + \frac{1}{Bu\Gamma^n} y_r \ ; \tag{5.1}$$

$$u = \cos\varphi + \epsilon^2 u_r + \cdots \ ,$$

$$v = -\sin\varphi + \epsilon v_r + \cdots \ ,$$

$$p = \Gamma p_r + \cdots \ , \tag{5.2}$$

$$\rho = 1 + \epsilon\rho_r + \cdots \ ,$$

$$T = \Gamma T_r + \cdots \ ,$$

$$I = 4I_r + \cdots \ .$$

Substitution of (5.1) and (5.2) into the equations of motion, (2.1)-(2.8), yields, to the leading order, the following:

$$
\begin{aligned}
& v_r - \rho_r \sin\varphi = 0, \qquad p_r = T_r \ , \\
& -\sin\varphi \frac{\partial v_r}{\partial y_r} + 2 \frac{\partial p_r}{\partial y_r} = 0 \ , \\
& -\sin\varphi \frac{\partial u_r}{\partial y_r} - 2Y'_r \frac{\partial p_r}{\partial y_r} = 0 \ , \qquad (5.3) \\
& -\sin\varphi \frac{\partial T_r}{\partial y_r} = \frac{4}{Bo} T_r^{\,n} (I_r - T_r^{\,4}) \ , \\
& \frac{\partial}{\partial y_r} \left(\frac{1}{T_r^{\,n}} \frac{\partial I_r}{\partial y_r} \right) = 3 T_r^{\,n} (I_r - T_r^{\,4}) \ .
\end{aligned}
$$

The energy equation retains the convection and radiation flux divergence terms with the pressure gradient, heat conduction, and viscous dissipation terms being of higher order.

The solutions to equations (5.3), in particular the energy and transfer equations, are difficult to find due to their nonlinearity. Although they are nonlinear, they can be solved since they can be transformed into a modified Bessel equation. By letting $\partial/\partial\eta = (1/T_r^{\,n})\, \partial/\partial y_r$ and combining the two equations one obtains:

$$
-\sin\varphi \frac{\partial T_r}{\partial \eta} = \frac{4}{3Bo} \frac{\partial^2 I_r}{\partial \eta^2} \ . \qquad (5.4)
$$

Integrating once and transforming from η to T_r as the independent variable, by use of the energy equation, yields:

$$K T_r = (I_r - T_r^4) \frac{\partial I_r}{\partial T_r} \tag{5.5}$$

where $K = 3Bo^2 \sin^2 \varphi / 16$. Letting $Z = T_r^2$ the equation becomes

$$\frac{dZ}{dI_r} = \frac{2}{K} (I_r - Z^2) \tag{5.6}$$

which is the Riccati equation. The Riccati equation can be transformed into the Airy equation (a modified Bessel equation) by letting $Z = (K/2)\, u'/u$, where $u' = du/dI_r$. Thus equation (5.6) becomes:

$$u'' - \frac{4}{K^2} I_r u = 0 \ . \tag{5.7}$$

The solution of the Airy equation is in terms of modified Bessel functions. Obtaining the solution of (5.7) and transforming back into temperature yields, after imposing the condition that $T_r \to 0$ as $I_r \to 0$:

$$T_r = \sqrt{I_r^{\frac{1}{2}} \frac{I_{2/3}\left[\frac{4}{3K} I_r^{3/2}\right]}{I_{-1/3}\left[\frac{4}{3K} I_r^{3/2}\right]}} \tag{5.8}$$

where the numerically subscripted I is a modified Bessel function and the letter subscripted I is the intensity.

Therefore the general solutions for the near precursor region, in terms of I_r, are:

$$T_r = \sqrt{I_r^{\frac{1}{2}} \frac{I_{2/3}\left[\frac{4}{3K} I_r^{3/2}\right]}{I_{-1/3}\left[\frac{4}{3K} I_r^{3/2}\right]}} \quad ,$$

$$p_r = T_r \quad ,$$

$$v_r = \frac{2}{\sin\varphi} T_r \quad , \tag{5.9}$$

$$\rho_r = \frac{2}{\sin^2\varphi} T_r \quad ,$$

$$u_r = -\frac{2\, Y_r'}{\sin\varphi} T_r \quad ,$$

$$y_r = -\frac{Bo \sin\varphi}{4} \int_0^{T_r} \frac{d\tau}{\tau^n (I_r - \tau^4)} \quad .$$

The solutions in the limit as $y_r \to \infty$ are:

$$p_r = T_r = \frac{1}{(\sqrt{3}\, n\, y_r)^{1/n}} + \cdots \quad ,$$

$$v_r = \frac{2}{\sin\varphi} T_r \quad ,$$

$$\rho_r = \frac{2}{\sin^2\varphi} T_r \quad , \tag{5.10}$$

$$u_r = -\frac{2Y_r'}{\sin\varphi} T_r \quad ,$$

$$I_r = \frac{\sqrt{3}\, Bo \sin\varphi}{4} \frac{1}{(\sqrt{3}\, n\, y_r)^{1/n}} + \cdots$$

and in the limit as $y_r \to 0$ are:

$$p_r = T_r = \theta_r(x_r) - \frac{4\theta_r^n}{Bo \sin\varphi} (J_r - \theta_r^4) y_r + \cdots ,$$

$$v_r = \frac{2}{\sin\varphi} T_r ,$$

$$\rho_r = \frac{2}{\sin^2\varphi} T_r , \tag{5.11}$$

$$u_r = - \frac{2Y_r'}{\sin\varphi} T_r ,$$

$$I_r = J_r(x_r) + b_r(x_r) \theta_r^n y_r + \cdots .$$

Applying the boundary conditions at $y_r = 0$, the following relations for J_r and b_r in terms of θ_r were found:

$$\theta_r = \sqrt{J_r^{\frac{1}{2}} \frac{I_{2/3}\left[\frac{4}{3K} J_r^{3/2}\right]}{I_{-1/3}\left[\frac{4}{3K} J_r^{3/2}\right]}} \tag{5.12}$$

and

$$b_r = - \frac{3 Bo \sin\varphi}{4} \theta_r .$$

The matching of the near-field precursor region to the interior region of the far-field precursor is done with respect to the normal coordinate, i.e., $\vec{\bar{y}}_2 = (- \epsilon Y_m + y)/\vec{\bar{\lambda}}_2$ where $Bu\vec{\bar{\lambda}}_2 \to 0$ and $Bu\Gamma^n \vec{\bar{\lambda}}_2 \to \infty$. The matchings are found to be identical, and thus no new constants are determined.

Numerical results of this region are also presented in Figure 4, in the form of a plot, along with the numerical results for the radiation relaxation region, to be discussed later. In this figure the fluid mechanical shock wave is represented by a discontinuity. These results can be compared to the results of Heaslet and Baldwin [11], for $\epsilon \neq 0$, given in Figure 1.

Chapter VI

THE OUTER REGION OF THE SHOCK STRUCTURE

The next region downstream from the near-field precursor region is the outer region of the shock structure. The scale thickness of this region is $O(\Gamma^{\omega}/R)$. This scale thickness is larger, by a factor Γ^{ω}, than the conventional outer region, since the temperature has risen to its shock layer order of magnitude in the near-field precursor due to the effectiveness of radiative transfer. In this region, all variables are scaled as constants plus small corrections. The fact that the pressure and temperature are varying as corrections to constant values, as opposed to variation as free variables, is the essential difference between this outer region and the conventional outer region. The coordinates and flow quantities, therefore, have the following representations:

$$x = x_o \quad , \qquad y = \epsilon\, Y_o(x_o) + \frac{\Gamma^{\omega}}{R}\, y_o \quad ; \tag{6.1}$$

$$u = \cos\varphi + \Omega^{1/P}\, u_o + \text{---} \quad ,$$

$$v = -\sin\varphi + \Omega^{3/4P}\, v_o + \text{---} \quad ,$$

$$p = \Gamma \left(\Pi_o(x_o) + \Omega\, p_o \right) + \text{---} \quad ,$$

$$\rho = 1 + \Omega^{3/4P}\, \rho_o + \text{---} \quad , \tag{6.2}$$

$$T = \Gamma \left(\theta_o(x_o) + \Omega\, T_o \right) + \cdots ,$$

$$I = 4 \left(J_o(x_o) + \Omega\, I_o \right) + \cdots ,$$

where $\Omega = Bu\Gamma^{n+\omega}/R$.

Substitution of (6.1) and (6.2) into the equations of motion, (2.1)-(2.8), yields to the leading order the following:

$$\Pi_o = \theta_o , \qquad p_o = T_o ,$$

$$v_o - \rho \sin\varphi = 0 ,$$

$$-\sin\varphi \frac{\partial v_o}{\partial y_o} + 2\epsilon\, \Omega^{1-3/4P} \frac{\partial p_o}{\partial y_o} = \frac{4}{3}\, \theta_o^{\omega} \frac{\partial^2 v_o}{\partial y_o^2} ,$$

$$-\sin\varphi \frac{\partial u_o}{\partial y_o} - 2\epsilon^2\, \Omega^{1-1/P}\, Y_o' \frac{\partial p_o}{\partial y_o} = \theta_o^{\omega} \frac{\partial^2 u_o}{\partial y_o^2} \qquad (6.3)$$

$$- \frac{1}{3}\, Y_o'\, \epsilon\, \Omega^{1/4P}\, \theta_o^{\omega} \frac{\partial^2 v_o}{\partial y_o^2} ,$$

$$-\sin\varphi \frac{\partial T_o}{\partial y_o} = \frac{\theta_o^{\omega}}{P} \frac{\partial^2 T_o}{\partial y_o^2} + \frac{4}{Bo}\, \theta_o^{n} (J_o - \theta_o^{4}) ,$$

$$\frac{1}{\theta_o^{n}} \frac{\partial^2 I_o}{\partial y_o^2} = 0 .$$

The solutions to (6.3) are:

$$p_o = T_o = S_o(x_o)\, A_o^{4P/3} \exp\left[-\frac{P \sin\varphi}{\theta_o^{\omega}} y_o\right]$$

$$- \frac{4\,\theta_o^{n}(J_o - \theta_o^{4})}{Bo \sin\varphi}\, y_o + \frac{4\,\theta_o^{n+\omega}(J_o - \theta_o^{4})}{Bo\, P \sin^2\varphi}$$

$$v_o = A_o \exp\left[-\frac{3\sin\varphi}{4\,\theta_o^{\omega}} y_o\right]$$

$$+ \varepsilon\, \Omega^{1-3/4P} \left\{\frac{3 S_o A_o^{4P/3}}{2\sin\varphi(\frac{3}{4} - P)} \exp\left[-\frac{P\sin\varphi}{\theta_o^{\omega}} y_o\right]\right.$$

$$\left. - \frac{8\,\theta_o^{n}(J_o - \theta_o^{4})}{Bo \sin^2\varphi}\, y_o + \frac{8\,\theta_o^{n+\omega}(J_o - \theta_o^{4})}{Bo \sin^3\varphi} (\tfrac{4}{3} + \tfrac{1}{P})\right\} ,$$

$$\rho_o = \frac{v_o}{\sin\varphi} \quad , \tag{6.4}$$

$$u_o = w_o(x_o)\, A_o^{4/3} \exp\left[-\frac{\sin\varphi}{\theta_o^{\omega}} y_o\right]$$

$$- \varepsilon\, \Omega^{1/4P}\, Y_o'\, A_o \exp\left[-\frac{3\sin\varphi}{4\,\theta_o^{\omega}} y_o\right]$$

$$- \varepsilon^2\, \Omega^{1-1/P}\, Y_o' \left\{\frac{2 S_o A_o^{4P/3}}{\sin\varphi(1-P)} \exp\left[-\frac{P\sin\varphi}{\theta_o^{\omega}} y_o\right]\right.$$

$$\left. - \frac{6\,\theta_o^{n}(J_o - \theta_o^{4})}{Bo \sin^2\varphi}\, y_o + \frac{6\,\theta_o^{n+\omega}(J_o - \theta_o^{4})}{Bo \sin^3\varphi} (1 + \tfrac{1}{P})\right\} ,$$

$$I_o = a_o + b_o\, \theta_o^{n}\, y_o \quad .$$

The matching of the outer region of the shock structure to the near-field precursor is performed using the normal coordinate as the matching variable, i.e., $\vec{\bar{y}}_3 = (-\epsilon Y_o + y)/\vec{\bar{\lambda}}_3$ where $Bu\Gamma^n \vec{\bar{\lambda}}_3 \to 0$ and $(\Gamma^\omega/R)\vec{\bar{\lambda}}_3 \to \infty$. During the course of the matchings it is found that

$$\theta_o(x_o) = \theta_r(x_r) \quad , \qquad J_o(x_o) = J_r(x_r)$$

and

$$b_o(x_o) = b_r(x_r) = -\frac{3Bo \sin\varphi}{4} \theta_r \quad . \tag{6.5}$$

It should be kept in mind that J_r and θ_r are not independent constants. It was also found, through the tangential velocity matching, that $Y_o' = 4/3\ Y_r'$. This is interesting, since this result implies that the near-field precursor region decreases in size as one proceeds away from the stagnation streamline. Stated more simply, the near-field precursor region is a radiation "cap" that sits ahead of the shock wave and becomes smaller in relative size as one moves along the shock away from the stagnation streamline and then finally disappears. Of course, the present theory breaks down at some point prior to the disappearance of the near-field precursor, since it is assumed that this region is to be of significant size.

Chapter VII

THE MIDDLE REGION OF THE SHOCK STRUCTURE

The next region downstream from the outer region of the shock structure is the middle region, or dissipation region, of the shock structure. The scale thickness of this middle region is $O(\Gamma^{\omega}/R)$, which is the same as for the outer region, but has an effective thickness which is much larger. The pressure and temperature are now free to adjust upwards, due to the fluid mechanical aspects of the shock wave. The velocity components and density are still of their freestream order of magnitude. The intensity is still scaled as a constant plus a correction, since the region is optically thin, which excludes any change of order one or greater. Thus, the coordinates and flow quantities, which (except for the intensity) are the same as for the nonradiating problem, have the following representations:

$$x = x_m \quad , \qquad y = \epsilon Y_m(x_m) + \frac{\Gamma^{\omega}}{R}\, y_m \quad ; \tag{7.1}$$

$$u = u_m + \text{---} \quad ,$$

$$v = v_m + \text{---} \quad ,$$

$$p = \Gamma p_m + \text{---} \quad , \tag{7.2}$$

$$\rho = \rho_m + \text{---} \quad ,$$

$$T = \Gamma T_m + \text{---} \quad ,$$

$$I = 4\left(J_m(x_m) + \frac{Bu\Gamma^{n+\omega}}{R} I_m\right) + \text{---} \quad .$$

Substitution of (7.1) and (7.2) into the equations of motion, (2.1)-(2.8), yields to the leading order the following:

$$p_m = \rho_m T_m \quad ,$$

$$\rho_m v_m = -\sin\varphi \quad ,$$

$$v_m \sin\varphi + \frac{4}{3} T_m^{\omega} \frac{\partial v_m}{\partial y_m} = -\sin^2\varphi \quad , \tag{7.3}$$

$$u_m \sin\varphi + T_m^{\omega} \frac{\partial u_m}{\partial y_m} = \cos\varphi \sin\varphi \quad ,$$

$$\sin\varphi \frac{\partial T_m}{\partial y_m} + \frac{1}{P} \frac{\partial}{\partial y_m}\left(T_m^{\omega} \frac{\partial T_m}{\partial y_m}\right) + T_m^{\omega}\left[\frac{4}{3}\left(\frac{\partial v_m}{\partial y_m}\right)^2 + \left(\frac{\partial u_m}{\partial y_m}\right)^2\right] = 0 \quad ,$$

$$\frac{\partial}{\partial y_m}\left(\frac{1}{\rho_m T_m^{\,n}} \frac{\partial T_m}{\partial y_m}\right) = 0 \quad .$$

Equations (7.3) are most easily solved by using a variable transformation. A modified Crocco transformation is used in which the independent variables (x_m, y_m) are changed to (x_m, V_m) where

$$V_m = v_m + \sin\varphi. \tag{7.4}$$

Equations (7.3) in terms of the new variables (x_m, V_m) are:

$$p_m = \rho_m T_m \quad , \qquad \rho_m v_m = -\sin\varphi \quad ,$$

$$\frac{\partial U_m}{\partial V_m} - \frac{4}{3}\frac{U_m}{V_m} = 0 \quad , \qquad U_m = u_m - \cos\varphi \quad ,$$

$$\frac{\partial^2 T_m}{\partial V_m^2} - \frac{(\frac{4}{3}P - 1)}{V_m}\frac{\partial T_m}{\partial V_m} + P\left[\frac{4}{3} + \left(\frac{\partial U_m}{\partial V_m}\right)^2\right] = 0 \quad , \tag{7.5}$$

$$\frac{\partial y_m}{\partial V_m} + \frac{4}{3}\frac{T_m^{\omega}}{V_m} = 0 \quad ,$$

$$\frac{\partial}{\partial V_m}\left(\frac{V_m}{\rho_m T_m^{n+\omega}}\frac{\partial I_m}{\partial V_m}\right) = 0 \quad .$$

The solutions to (7.5) are:

$$\rho_m = \frac{\sin\varphi}{v_m} \quad ,$$

$$u_m = \cos\varphi + w_m(x_m)\left[\sin\varphi + v_m\right]^{4/3} \quad ,$$

$$T_m = \Theta_m(x_m) + S_m(x_m)\left[\sin\varphi + v_m\right]^{4P/3} - \frac{P}{3-2P}\left[\sin\varphi + v_m\right]^2 - \frac{P w_m^2}{2(2-P)}\left[\sin\varphi + v_m\right]^{8/3} \quad , \tag{7.6}$$

$$p_m = \rho_m T_m \quad ,$$

$$y_m = L_m - \frac{4}{3\sin\varphi}\int_{-\sin\varphi + A_m}^{v_m} \frac{T_m^{\omega}}{\sin\varphi + v}\, dv \quad ,$$

$$I_m = a_m(x_m) - \frac{4\, b_m(x_m)}{3\sin\varphi} \int_{-\sin\varphi + A_m}^{v_m} \frac{T_m^{n+\omega}}{\sin\varphi + v}\, dv .$$

where now θ_m appears in the solution to the temperature. It is needed since the gas is preheated due to the precursor effect.

The matching of this middle region to the outer region of the shock structure is most conveniently done with respect to the normal coordinate, i.e., $\vec{\bar{y}}_4 = (-\epsilon Y_m - K_m Z_m + y)\vec{\bar{\lambda}}_4$ where $(R/\Gamma^{(\omega)})\vec{\bar{\lambda}}_4 \to \infty$ and $(R/\Gamma^{(\omega)})K_m Z_m \gg (R/\Gamma^{(\omega)})\vec{\bar{\lambda}}_4$. It is also required that $(\epsilon R/\Gamma^{(\omega)})\vec{\bar{\lambda}}_4 \to 0$ so that the normal and tangential velocity components will match for $P \geq \frac{3}{4}$. To perform the matchings, the solutions of equations (7.6) in terms of (x_m, y_m) as $y_m \to (R/\Gamma^{(\omega)})K_m Z_m \to \infty$ are found to be:

$$\rho_m = \frac{\sin\varphi}{\sin\varphi - A_m(x_m) \exp - \dfrac{3\sin\varphi}{4\,\theta_m^{\omega}}\, y_m} ,$$

$$u_m = \cos\varphi + w_m A_m^{4/3} \exp - \frac{\sin\varphi}{\theta_m^{\omega}}\, y_m ,$$

$$T_m = \theta_m + S_m A_m^{4P/3} \exp - \frac{P\sin\varphi}{\theta_m^{\omega}}\, y_m ,$$

$$p_m = \rho_m T_m ,$$

$$v_m = -\sin\varphi + A_m \exp - \frac{3\sin\varphi}{4\,\theta_m^{\omega}}\, y_m ,$$

$$I_m = a_m + b_m\, \theta_m^{n}\, y_m .$$

Performing the matchings it is found that

$$J_m(x_m) = J_o(x_o) = J_r(x_r) \ ,$$

$$\Theta_m(x_m) = \Theta_o(x_o) = \Theta_r(x_r) \ , \qquad (7.8)$$

$$S_m(x_m) = S_o(x_o) \ , \quad A_m(x_m) = A_o(x_o) \ ,$$

$$b_m(x_m) = b_o(x_o) = -\frac{3Bo \sin\varphi}{4} \Theta_r \ .$$

It is also found that the restriction for matching on the Prandtl number of $\frac{1}{2} < P < \frac{3}{2}$ is required as it was for the nonradiating problem. The effective thickness is found to be $Z_m = (\Gamma^{\omega}/R)\log R/Bu\Gamma^{n+\omega}$ with $K_m = \Theta_m^{\omega}/P\sin\varphi$.

Chapter VIII

THE INNER REGION OF THE SHOCK STRUCTURE

The next region of the shock structure is the inner region which is thinner than the middle region by a factor ϵ. The tangential velocity component and temperature have already reached their stagnation orders of magnitude and are therefore scaled as corrections to their middle region values. The density finally rises to its stagnation order of magnitude, which must be accompanied by a corresponding rise in pressure and a decrease in the normal velocity component. The intensity is again scaled as constant plus a small correction, since this region is also optically thin. The coordinates and flow quantities in this inner region have the following forms:

$$x = x_i \,, \qquad y = \epsilon Y_i(x_i) + \frac{\epsilon \Gamma^{(\omega)}}{R}\, y_i \,; \tag{8.1}$$

$$u = W_i(x_i) + \epsilon u_i + \text{---} \,,$$

$$v = \epsilon v_i + \text{---} \,,$$

$$p = (\Gamma/\epsilon) p_i + \text{---} \,,$$

$$\rho = (1/\epsilon)\rho_i + \text{---} \,, \tag{8.2}$$

$$T = \Gamma\left(\theta_i(x_i) + \varepsilon T_i\right) + \text{---} \ ,$$

$$I = 4\left(J_i(x_i) + \Omega I_i\right) + \text{---} \ .$$

The equations of motion (2.1)-(2.8) consistent with the above expansions are:

$$p_i = \rho_i \theta_i \ , \qquad \rho_i V_i = -\sin\varphi \ ,$$

$$-2\sin\varphi \frac{\theta_i}{V_i} - \frac{4}{3} \theta_i^{\omega} \frac{\partial V_i}{\partial y_i} = \sin^2\varphi \ ,$$

$$\theta_i^{\omega} \frac{\partial u_i}{\partial y_i} = \sin\varphi \left(\cos\varphi - W_i\right) \ , \tag{8.3}$$

$$\frac{\theta_i^{\omega}}{P} \frac{\partial T_i}{\partial y_i} = \sin\varphi \left[\left(\tfrac{1}{2}\sin^2\varphi - \theta_i + \theta_m\right) + \tfrac{1}{2}\left(\cos\varphi - W_i\right)^2\right] \ ,$$

$$\frac{\partial}{\partial y_i}\left(\frac{1}{\rho_i \theta_i^{\,n}} \frac{\partial I_i}{\partial y_i}\right) = 0 \ .$$

where $V_i = v_i - Y_i' W_i$. The solutions to these equations are:

$$\rho_i = -\frac{\sin\varphi}{V_i} \ ,$$

$$p_i = \rho_i \theta_i \ ,$$

$$u_i = w_i(x_i) - \sin\varphi \left(\cos\varphi - W_i\right) \frac{\left\{Y_i(x_i) - y_i\right\}}{\theta_i^{\omega}} \ , \tag{8.4}$$

$$T_i = S_i(x_i) - P\sin\varphi\left[\left(\tfrac{1}{2}\sin^2\varphi - \theta_i + \theta_m\right) + \tfrac{1}{2}(\cos\varphi - W_i)^2\right]\frac{\{Y_i - y_i\}}{\theta_i^{\omega}} \quad ,$$

$$I_i = a_i(x_i) + \frac{4\theta_i^{n+\omega}}{3\sin\varphi}\left(\log\left|\, V_i + \frac{2\theta_i}{\sin\varphi}\,\right|\right) \quad ,$$

$$\left|\sin^2\varphi\,\left(V_i + \frac{2\theta_i}{\sin\varphi}\right)\right| = \exp\left[\frac{\sin\varphi}{2\theta_i}\left(V_i + \frac{2\theta_i}{\sin\varphi}\right) - \frac{3}{8}\frac{\sin^3\varphi}{\theta_i^{1+\omega}}\{Y_i - y_i\}\right].$$

The matching of the inner region to the middle region is most easily accomplished by using the normal velocity as the matching variable, i.e., $\vec{\vec{v}}_5 = v/\vec{\vec{\beta}}_5$ where $\vec{\vec{\beta}}_5 \to 0$ and $\vec{\vec{\beta}}_5/\varepsilon \to \infty$. In performing the matchings, it is found that:

$$J_i(x_i) = J_m(x_m) = J_r(x_r) \quad ,$$

$$b_i(x_i) = b_m(x_m) = -\frac{3Bo\,\sin\varphi}{4}\,\theta_r(x_r) \quad ,$$

$$a_m(x_m) = \frac{4b_r(x_r)}{3\sin\varphi}\int_{-\sin\varphi + A_o}^{-\varepsilon}\frac{\rho_m T_m^{n+\omega}}{\sin\varphi + v_m}\,dv_m \quad , \tag{8.5}$$

$$w_m(x_m) = -\frac{(\cos\varphi - W_i)}{(\sin\varphi)^{4/3}} \quad ,$$

and

$$S_m(x_m) = \frac{\theta_i - \theta_m + \frac{P}{3-2P}\sin^2\varphi + \frac{P}{2(2-P)}(\cos\varphi - W_i)}{(\sin\varphi)^{4P/3}} \quad .$$

Chapter IX

THE RADIATION RELAXATION REGION

The region that follows the inner region of the shock structure is the radiation relaxation region. This region was not present in the nonradiating problem, since there was no need for a region in which radiative equilibration would occur. The rise of radiative intensity in this region is accompanied by a decrease of temperature, Heaslet and Baldwin [11]. This decrease in temperature, or cooling of the gas, is referred to as radiative cooling. This transfer of energy, in the form of temperature, out of this region is responsible for the precursor temperature rise before the shock wave. The flow quantities in this region have all reached their shock layer order of magnitude, and are therefore scaled as such. The scale thickness of this relaxation region is of the order of the photon mean free path at shock layer conditions and is thus equal to $O(\epsilon/Bu\Gamma^n)$. As this region is mainly a radiation-dominated one, it would be expected that all three terms of the transfer equation are present; i.e., gradient, absorption and emission terms. This is, in fact, the case, as will be seen in the equations.

The coordinates and flow quantities which describe this radiation relaxation region are:

$$x = x_a \quad , \qquad y = \epsilon Y_a(x_a) + \frac{\epsilon}{Bu\Gamma^n} y_a \quad ; \tag{9.1}$$

$$u = W_a + \epsilon^2 u_a + \text{---} \quad ,$$

$$v = \epsilon v_a + \text{---} \quad ,$$

$$p = \frac{\Gamma}{\epsilon}\left(\Pi_a + \epsilon p_a\right) + \text{---} \quad , \tag{9.2}$$

$$\rho = \frac{1}{\epsilon}\rho_a + \text{---} \quad ,$$

$$T = \Gamma T_a + \text{---} \quad ,$$

$$I = 4I_a + \text{---} \quad .$$

Substitution of equations (9.1) and (9.2) into the equations of motion, (2.1)-(2.8), yields:

$$\frac{\partial}{\partial y_a}(\rho_a v_a) - Y_a' \frac{\partial}{\partial y_a}(\rho_a W_a) = 0 \quad ,$$

$$-\sin\varphi \frac{\partial u_a}{\partial y_a} - 2Y_a' \frac{\partial p_a}{\partial y_a} = 0 \quad ,$$

$$-\sin\varphi \frac{\partial v_a}{\partial y_a} + 2 \frac{\partial p_a}{\partial y_a} = 0 \quad , \qquad \Pi_a = \rho_a T_a \quad , \tag{9.3}$$

$$-\sin\varphi \frac{\partial T_a}{\partial y_a} = \frac{4}{Bo} \rho_a T_a^{\,n} (I_a - T_a^{\,4}) \quad ,$$

$$\frac{\partial}{\partial y_a}\left(\frac{1}{\rho_a T_a^{\,n}} \frac{\partial I_a}{\partial y_a}\right) = 3 \rho_a T_a^{\,n} (I_a - T_a^{\,4}) \quad .$$

The solution to these equations was carried out numerically and a representative solution is shown in Figure 4, as mentioned before.

In order that upstream and downstream matchings might be obtained, the solutions in these limits must be found. The solutions in the upstream limit, as $y_a \to Y_a$, are:

$$
\begin{aligned}
I_a &= J_a(x_a) + b_a(x_a)\ \Pi_a\ \theta_a^{n-1}\ (y_a - Y_a) \quad , \\
T_a &= \theta_a - \frac{2\sin\varphi}{Bo}\ \theta_a^{n-1}\ (J_a - \theta_a^4)\ (y_a - Y_a) \quad , \\
p_a &= \tfrac{1}{2}\ (c_1 - v_a \sin\varphi) \quad , \\
\rho_a &= \frac{\Pi_a}{T_a} \quad , \\
u_a &= -\frac{1}{\sin\varphi}\ (c_2 + 2Y'_a\ p_a) \quad , \\
v_a &= -\frac{\sin\varphi}{\rho_a} + Y'_a\ W_a \quad .
\end{aligned}
\tag{9.4}
$$

and the solutions in the downstream limit, as $y_a \to -\infty$, are:

$$
\begin{aligned}
I_a &= \theta_B^4\ (x_a) - B(x_a)\ \exp\ \sqrt{3}\ (\frac{\sin^2\varphi}{2}\ \theta_B^{n-1})y_a \quad , \\
T_a &= \theta_B + \frac{4B}{\sqrt{3}\ Bo\ \sin\varphi}\ \exp\ \sqrt{3}\ (\frac{\sin^2\varphi}{2}\ \theta_B^{n-1})y_a \quad , \\
p_a &= \tfrac{1}{2}\ (c_1 - v_a \sin\varphi) \quad , \\
\rho_a &= \frac{\Pi_a}{T_a} \quad ,
\end{aligned}
\tag{9.5}
$$

$$u_a = - \frac{1}{\sin\varphi} \left(c_2 + 2Y'_a \, p_a \right) \quad ,$$

$$v_a = - \frac{\sin\varphi}{\rho_a} + Y'_a \, W_a \quad .$$

The matching of the radiation relaxation region to the inner region of the shock structure is accomplished using the normal coordinate as the matching variable, i.e., $\vec{\vec{y}}_6 = (\epsilon Y_a - y)\vec{\vec{\lambda}}_6$ where $(R/\epsilon\Gamma^{(\omega)})\vec{\vec{\lambda}}_6 \to \infty$ and $(Bu\Gamma^n/\epsilon)\vec{\vec{\lambda}}_6 \to 0$. The matching establishes the upstream boundary conditions for the radiation relaxation region, and therefore this matching finds the "fluid-mechanical" shock conditions. (It should be noted, as mentioned before, that strict matching for these two regions was not accomplished since higher order terms must be included. The reader is again referred to Bush [4] for this matching.) Through performing these matchings the following relationships are found:

$$\theta_a(x_a) = \theta_i(x_i) = \frac{\sin^2\varphi}{2} + \theta_m \quad ,$$

$$W_a(x_a) = W_i(x_i) = \cos\varphi \quad , \tag{9.6}$$

$$\Pi_a(x_a) = \frac{\sin^2\varphi}{2} \quad , \quad J_a(x_a) = J_i(x_i) = J_r(x_r) \quad ,$$

and

$$b_a(x_a) = b_i(x_i) = - \frac{3 \, Bo \sin\varphi}{4} \theta_r \quad .$$

An interesting result is that the pressure is constant, to leading order, in this region. This fact was first realized by Goulard [10], and later discussed by Penner and Olfe [16]. It should also be noted

that the tangential velocity and pressure have attained their Rankine-Hugoniot conditions at the start of this region, whereas the temperature is above the Rankine-Hugoniot value of $\sin^2\varphi/2$ by θ_m. Since θ_m is also equal to the amount of temperature rise before the shock, due to precursor radiation, it can be seen that the temperature jump across the fluid mechanical shock only is Rankine-Hugoniot to the leading order. In other words, the temperature jump across the shock is $\sin^2\varphi/2$, i.e., from θ_m to $\theta_m + \sin^2\varphi/2$. In the present analysis the equations of motion in the radiation shock structure and fluid mechanical shock structure are one-dimensional, and consequently the conservation of mass, momentum, and energy must be maintained in the normal direction. This fact means that the jump conditions across the radiation shock (with the fluid mechanical shock imbedded within) must also be Rankine-Hugoniot, i.e., a temperature jump from 0 to $\sin^2\varphi/2$. Therefore the downstream value for the temperature, θ_B, is given by:

$$\theta_B = \theta_i - \theta_m = \frac{\sin^2\varphi}{2} \quad . \tag{9.7}$$

In this analysis the radiation and fluid mechanical shock structures were one-dimensional, as mentioned above, as a consequence of the assumption that $1/Bu\Gamma^n \ll 1$. If, on the other hand, the assumption of $1/bu\Gamma^n = O(1)$ were made, the radiation structure would become two-dimensional. Two-dimensionality in the radiation structure allows transfer of energy in the longitudinal direction. Therefore, conservation of energy in the normal direction is therefore no longer a

requirement, and this manifests itself in that the Rankine-Hugoniot conditions across the radiation structure are no longer valid. The jump conditions across the radiation structure are less severe with energy loss in the longitudinal direction. It should be noted from physical considerations that the fluid mechanical shock structure, imbedded within the radiation shock structure, is still one-dimensional under the assumption of $1/Bu\Gamma^n = O(1)$. Therefore, Rankine-Hugoniot jump conditions across the imbedded fluid mechanical shock structure apply locally in both the one-dimensional and two-dimensional cases, although the initial and final conditions are different. In the two-dimensional case, the radiation relaxation region thickness is $O(\epsilon/Bu\Gamma^n) = O(\epsilon)$, which is equivalent to the thickness of the shock layer, and therefore the radiation relaxation region extends all the way to the body and has terms common to both the radiation relaxation region and shock layer in the one-dimensional case.

Chapter X

THE SHOCK LAYER

The region between the radiation relaxation region and the body is the shock layer and it is inviscid, since $K = \Gamma^{\omega}/\epsilon R \to 0$. In the case under consideration, the shock layer is in radiative equilibrium and the orders of magnitude as determined by Bush [3], Chester [5], and Freeman [7] are appropriate. Thus the coordinates and flow quantities have the following forms:

$$x = x_L \quad , \qquad y = \epsilon y_L \quad ; \tag{10.1}$$

$$\begin{aligned} u &= u_L + \text{---} \quad , & v &= \epsilon v_L + \text{---} \quad , \\ p &= \frac{\Gamma}{\epsilon} p_L + \text{---} \quad , & \rho &= \frac{1}{\epsilon} \rho_L + \text{---} \quad , \\ T &= \Gamma T_L + \text{---} \quad , & I &= 4 I_L + \text{---} \quad , \end{aligned} \tag{10.2}$$

The leading terms in the equations of motion (2.1)-(2.8), consistent with the above expansions, are:

$$\begin{aligned} & p_L = \rho_L T_L \quad , \\ & \frac{\partial}{\partial x_L} (B \rho_L u_L) + \frac{\partial}{\partial y_L} (B \rho_L v_L) = 0 \quad , \\ & 2 \frac{\partial p_L}{\partial y_L} - \kappa \rho_L u_L^2 = 0 \quad , \end{aligned} \tag{10.3}$$

$$\rho_L \left(u_L \frac{\partial u_L}{\partial x_L} + v_L \frac{\partial u_L}{\partial y_L}\right) = 0 \quad ,$$

$$\rho_L \left(u_L \frac{\partial T_L}{\partial x_L} + v_L \frac{\partial T_L}{\partial y_L}\right) = 0 \quad ,$$

$$I_L = T_L^4 \quad .$$

A transformation of variables from (x_L, y_L) to (s_L, t_L) where

$$s_L = x_L \quad , \qquad t_L = \frac{u_L}{\cos\varphi} = \frac{u_L}{\sigma}$$

and

$$t_L = \left(\frac{T_L}{B}\right)\left(\frac{\partial u_L}{\partial y_L}\right)$$

yields the following solutions for the inviscid shock layer:

$$T_L = \tfrac{1}{2}\left[1 - t_L^2\sigma^2\right] ,$$

$$p_L = \tfrac{1}{2}\left[(1 - \sigma^2) - \frac{\kappa(\sigma)}{B(\sigma)} \int_{t_L\sigma}^{\sigma} \frac{\nu B(\nu)}{\kappa(\nu)}\, d\nu\right] ,$$

$$\tau_L = \frac{t_L\sigma\ \kappa(t_L\sigma)}{B(t_L\sigma)} \frac{p_L}{T_L^{1-\omega}} \quad , \tag{10.4}$$

$$y_L = \frac{1}{B(\sigma)(1-\sigma^2)} \int_0^{\tau_L} \frac{(1 - \sigma^2\nu^2)\ B(\sigma\nu)\ d\nu}{\nu\,\kappa(\sigma\nu)\left[1 - \dfrac{\kappa(\sigma)}{B(\sigma)(1-\sigma^2)} \displaystyle\int_{\sigma\nu}^{\sigma} \frac{hB(h)}{\kappa(h)}\, dh\right]} ,$$

$$I_L = \frac{1}{16}\left(1 - t_L^2\,\sigma^2\right)^4$$

The matching of the shock layer to the radiation relaxation region was carried using the matching variable $\vec{\bar{y}}_7 = (\epsilon Y_L - y)/\vec{\bar{\lambda}}_7$ where $(Bu\Gamma^n/\epsilon)\vec{\bar{\lambda}}_7 \to \infty$ and $\vec{\bar{\lambda}}_7/\epsilon \to 0$. These matchings give the "radiative" shock conditions. Thus the shock layer boundary conditions were found to be:

$$\begin{aligned}
u_L\,(x_L, Y_L) &= W_a(x_a) = \cos\varphi\ , \\
p_L\,(x_L, Y_L) &= \Pi(x_a) = \frac{\sin^2\varphi}{2}\ , \\
\rho_L\,(x_L, Y_L) &= 1\ , \\
T_L\,(x_L, Y_L) &= \frac{\sin^2\varphi}{2}\ , \\
v_L\,(x_L, Y_L) &= Y_L'\cos\varphi - \sin\varphi\ , \\
I_L\,(x_L, Y_L) &= \frac{\sin^8\varphi}{16}\ .
\end{aligned} \tag{10.5}$$

Chapter XI

THE BODY LAYER

The coordinates and expansion appropriate for the body layer are:

$$x = x_c \quad , \qquad y = \epsilon^{3/2} y_c \quad ; \tag{11.1}$$

$$u = \epsilon^{1/2} u_c + \text{---} \quad ,$$

$$v = \epsilon^{2} v_c + \text{---} \quad ,$$

$$p = \frac{\Gamma}{\epsilon} p_c + \text{---} \quad , \tag{11.2}$$

$$\rho = \frac{1}{\epsilon} \rho_c + \text{---} \quad ,$$

$$T = \Gamma T_c + \text{---} \quad ,$$

$$I = 4I_c + \text{---} \quad .$$

The equations of motion consistent with the above expansions are:

$$p_c = \rho_c T_c \quad ,$$

$$\frac{\partial}{\partial x_c} (B \rho_c u_c) + \frac{\partial}{\partial y_c} (B \rho_c v_c) = 0 \quad ,$$

$$\frac{\partial p_c}{\partial y_c} = 0 \quad , \tag{11.3}$$

$$\rho_c \left(u_c \frac{\partial u_c}{\partial x_c} + v_c \frac{\partial u_c}{\partial y_c}\right) + 2 \frac{\partial p_c}{\partial x_c} = D \frac{\partial}{\partial y_c} \left(T_c^{\omega} \frac{\partial u_c}{\partial y_c}\right) \quad ,$$

$$\rho_c \left(u_c \frac{\partial T_c}{\partial x_c} + v_c \frac{\partial T_c}{\partial y_c}\right) = \frac{D}{P} \frac{\partial}{\partial y_c} \left(T_c^{\omega} \frac{\partial T_c}{\partial y_c}\right) \quad ,$$

$$I_c = T_c^4 \quad ,$$

where

$$D = \frac{\Gamma^{\omega}}{\epsilon^{5/2} R} \quad .$$

The boundary conditions, obtained from the matching of the body layer to the inviscid shock layer, in Crocco variables ($s_c = x_c$, $t_c = u_c/\cos\varphi$, $\tau_c = \{T_c^{\omega}/B\}\{\partial u_c/\partial y_c\}$), are:

$$p_c (s_c, t_c \to \infty) = p_c(s_c) \quad ,$$

$$T_c (s_c, t_c \to \infty) = \tfrac{1}{2} \quad ,$$

$$\tau_c (s_c, t_c \to \infty) = 2^{1-\omega} p_c(s_c) \quad , \qquad (11.4)$$

$$I_c (s_c, t_c \to \infty) = \frac{1}{16} \quad .$$

The solutions to equations (11.3) for the inviscid case, $D \to 0$, consistent with boundary conditions (11.4) are:

$$p_c (s_c, t_c) = p_c(s_c) \quad ,$$

$$T_c (s_c, t_c) = \tfrac{1}{2} \quad ,$$

$$
\begin{aligned}
\tau_c\,(s_c,t_c) &= 2^{1-\omega}\; p_c(s_c) \quad , \\
y_c\,(s_c,t_c) &= \frac{\cos\varphi}{2B(s_c)p_c(s_c)}\left[t_c - t_{c,w}\,(s_c)\right] \quad , \qquad (11.5) \\
I_c\,(s_c,t_c) &= \frac{1}{16} \quad , \\
t_{c,w}\,(s_c) &= \frac{\left[-2\,\ln\{2\,p_c(s_c)\}\,\right]^{\frac{1}{2}}}{\cos\varphi} \quad .
\end{aligned}
$$

The boundary conditions for the viscous body layer are satisfied in the same way as done by Bush [3]. However, since the viscous body layer solutions are numerical, they will not be presented here.

Chapter XII

THE VISCOUS BOUNDARY LAYER

The coordinates and flow quantities for the viscous boundary layer are:

$$x = x_{BL} \quad , \qquad y = \left(\frac{\epsilon^{\frac{1}{2}} \Gamma^{\omega}}{R} \right)^{\frac{1}{2}} y_{BL} \quad ; \tag{12.1}$$

$$u = \epsilon^{\frac{1}{2}} u_{BL} + \text{---} \quad ,$$

$$v = \left(\frac{\epsilon^{3/2} \Gamma^{\omega}}{R} \right)^{\frac{1}{2}} v_{BL} + \text{---} \quad ,$$

$$p = \frac{\Gamma}{\epsilon} p_{BL} + \text{---} \quad , \tag{12.2}$$

$$\rho = \frac{1}{\epsilon} \rho_{BL} + \text{---} \quad ,$$

$$T = \Gamma T_{BL} + \text{---} \quad ,$$

$$I = 4 I_{BL} + \text{---} \quad .$$

The equations of motion resulting from the above expansions are:

$$p_{BL} = \rho_{BL} T_{BL} \quad ,$$

$$\frac{\partial}{\partial x_{BL}} (B \rho_{BL} u_{BL}) + \frac{\partial}{\partial y_{BL}} (B \rho_{BL} v_{BL}) = 0 \quad , \tag{12.3}$$

$$\frac{\partial p_{BL}}{\partial y_{BL}} = 0 \quad ,$$

$$\rho_{BL}\left(u_{BL}\frac{\partial u_{BL}}{\partial x_{BL}} + v_{BL}\frac{\partial u_{BL}}{\partial y_{BL}}\right) + 2\frac{\partial p_{BL}}{\partial x_{BL}} = \frac{\partial}{\partial y_{BL}}\left(T_{BL}^{\omega}\frac{\partial u_{BL}}{\partial y_{BL}}\right) \quad ,$$

$$\rho_{BL}\left(u_{BL}\frac{\partial T_{BL}}{\partial x_{BL}} + v_{BL}\frac{\partial T_{BL}}{\partial y_{BL}}\right) = \frac{1}{P}\frac{\partial}{\partial y_{BL}}\left(T_{BL}^{\omega}\frac{\partial T_{BL}}{\partial y_{BL}}\right) \quad ,$$

$$I_{BL} = T_{BL}^{4} \quad .$$

The boundary conditions at the outer edge of the boundary layer, obtained from matching with the inviscid body layer, are:

$$T_{BL}\left(x_{BL}, y_{BL} \to \infty\right) = \tfrac{1}{2} \quad ,$$

$$p_{BL}\left(x_{BL}, y_{BL} \to \infty\right) = p_{BL}(x_{BL}) = p_c(x_c) \quad , \qquad (12.4)$$

$$u_{BL}\left(x_{BL}, y_{BL} \to \infty\right) = \left[-2\ln\left\{2p_c(x_c)\right\}\right]^{\frac{1}{2}} \quad ,$$

$$I_{BL}\left(x_{BL}, y_{BL} \to \infty\right) = \frac{1}{16} \quad .$$

REFERENCES

1. Bond, John W., Kenneth M. Watson and Jasper A. Welch, Jr., Atomic Theory of Gas Dynamics, Addison-Wesley, (1956).
2. Burggraf, Odus R., "Asymptotic Solution for the Viscous Radiating Shock Layer," AIAA Journal, Vol. 4, No. 10, pp. 1725-1734, (1966).
3. Bush, William B., "On the Viscous Hypersonic Blunt Body Problem," Journal of Fluid Mechanics, Vol. 20, part 3, pp. 353-367, (1964).
4. Bush, W. B., "An Asymptotic Analysis of Radiation-Resisted Shock Waves," (to be published).
5. Chester, W , "Supersonic Flow Past a Bluff Body with a Detached Shock: Part II. Axisymmetric Body," Journal of Fluid Mechanics, Vol. 1, part 5, pp. 490-496, (1956).
6. Emanuel, George, "Application of Matched Asymptotic Expansions to Radiative Transfer in an Optically Thick Gas," Heat Transfer and Fluid Mechanics Institute, Stanford University Press, (1972).
7. Freeman, N. C., "On the Theory of Hypersonic Flow Past Plane and Axially Symmetric Bluff Bodies," Journal of Fluid Mechanics, Vol. 1, part 4, pp. 366-387, (1956).
8. Goulard, R., "Similarity Parameters in Radiation Gas-Dynamics," High Temperature in Aeronautics, edited by C. Ferrari, Pergamon, (1964).

9. Goulard, R., "Preliminary Estimates of Radiative Transfer Effects on Detached Shock Layers," AIAA Journal, Vol. 2, No. 3, pp. 494-502, (1964).

10. Goulard, R., Supersonic Flow, Chemical Processes and Radiation, edited by D. B. Olfe and V. Zakkay, Pergamon, (1964).

11. Heaslet, M. A., and B. S. Baldwin, "Predictions of the Structure of Radiation-Resisted Shock Waves," Physics of Fluids, Vol. 6, No. 6, pp. 781-791, (1963).

12. Jische, Martin C., "Optically Thin Stagnation-Point Flow," AIAA Journal, Vol. 6, No. 11, pp. 2219-2222, (1968).

13. Liu, J. T. C., Reply by author to W. Schneider, AIAA Journal, Vol. 8, No. 6, p. 1181, (1970).

14. Nelson, H. F., and R. Goulard, "Structure of Shock Waves with Non-equilibrium and Ionization," Physics of Fluids, Vol. 12, No. 8, pp. 1605-1614, (1969).

15. Olfe, D. B., "Radiative Cooling in Transparent Shock Layers of Wedges and Cones," AIAA Journal, Vol. 4, No. 10, pp. 1734-1740, (1966).

16. Penner, S. S., and Daniel B. Olfe, Radiation and Reentry, Academic Press, (1968).

17. Schneider, W., Comment on "Radiative Transfer in Low Reynolds Number, Blunt-Body Stagnation Region at Hypersonic Speeds," AIAA Journal, Vol. 8, No. 6, pp. 1180-1181, (1970).

18. Thomas, P. D., "Air Emissivity and Shock Layer Radiation," Journal of Aerospace Sciences, Vol. 29, No. 5, pp. 362-368, (1962).

19. Traugott, S. C., "A Differential Approximation for Radiative Transfer with Application to Normal Shock Structure," Heat Transfer and Fluid Mechanics Institute, Stanford University Press, (1963).

20. Traugott, S. C., "Shock Structure in a Radiating, Heat Conducting, and Viscous Gas," Physics of Fluids, Vol. 8, No. 5, pp. 834-849, (1965).

21. Vincenti, Walter G., and Charles H. Kruger, Jr., Introduction to Physical Gas Dynamics, John Wiley and Sons, (1965).

22. Zel'dovich, Ya. B., and Yu. P. Raizer, Physics of Shock Waves and High-Temperature Hydrodynamic Phenomena, edited by Wallace D. Hayes and Ronald F. Probstein, Academic Press, (1966).

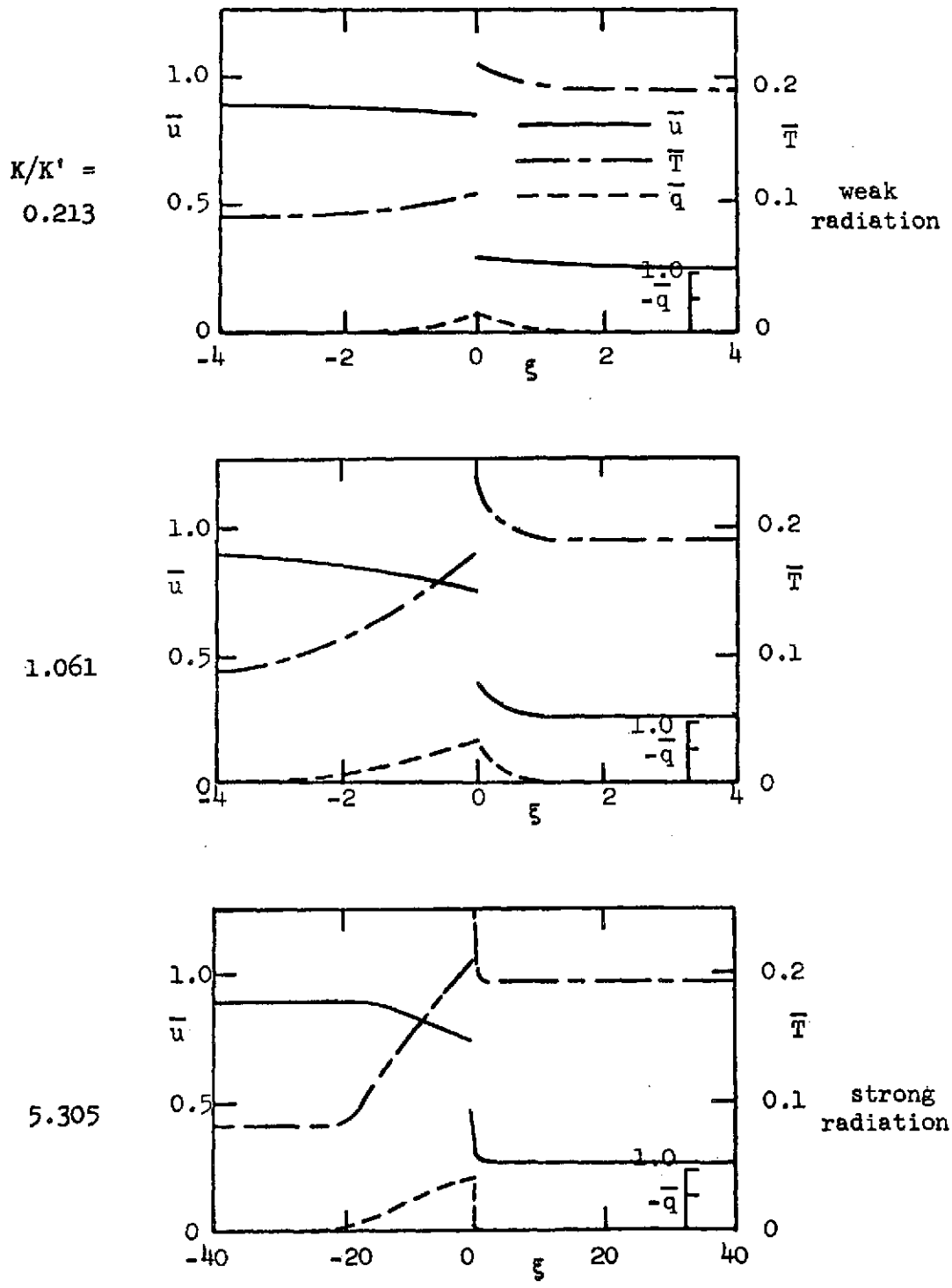

Figure 1. Results of Heaslet and Baldwin [11] for the strong shock case.

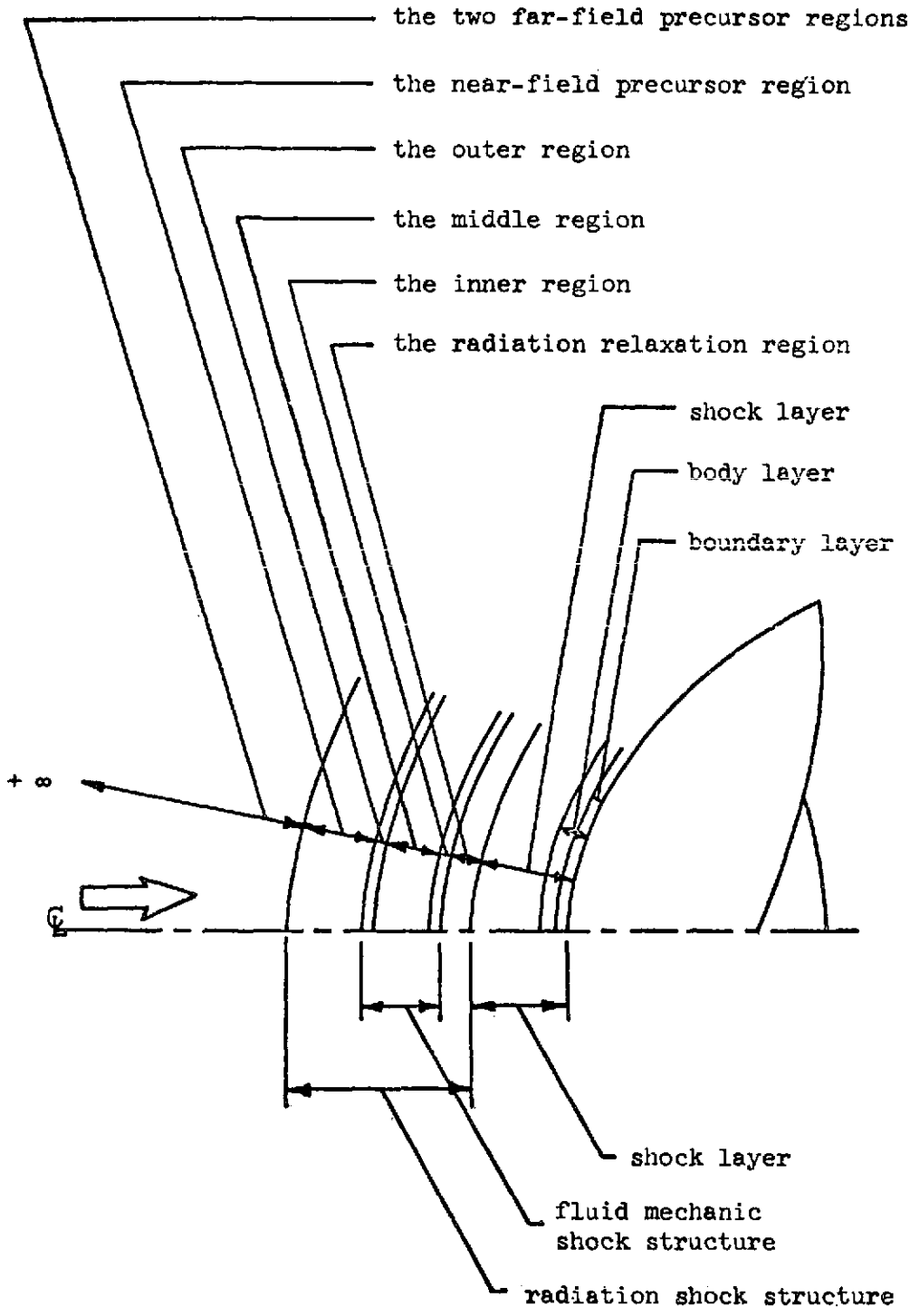

Figure 2. Schematic of the regions of flow.

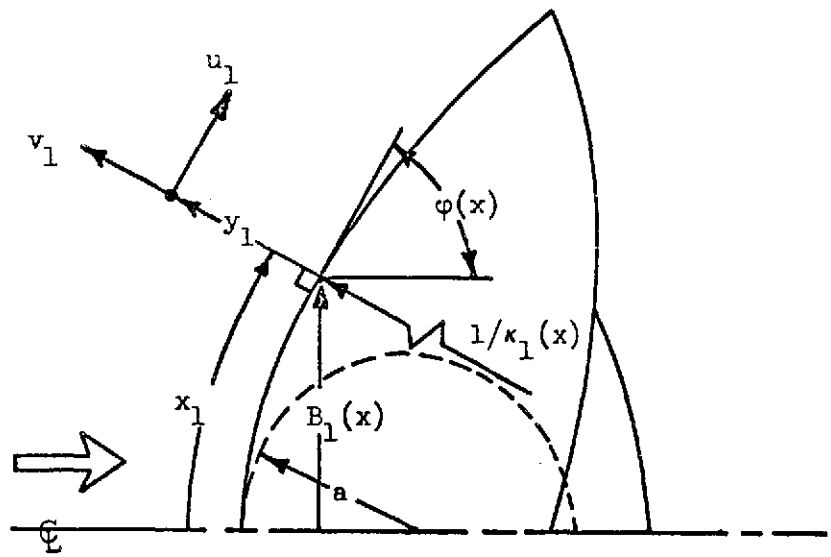

Figure 3. The coordinate system.

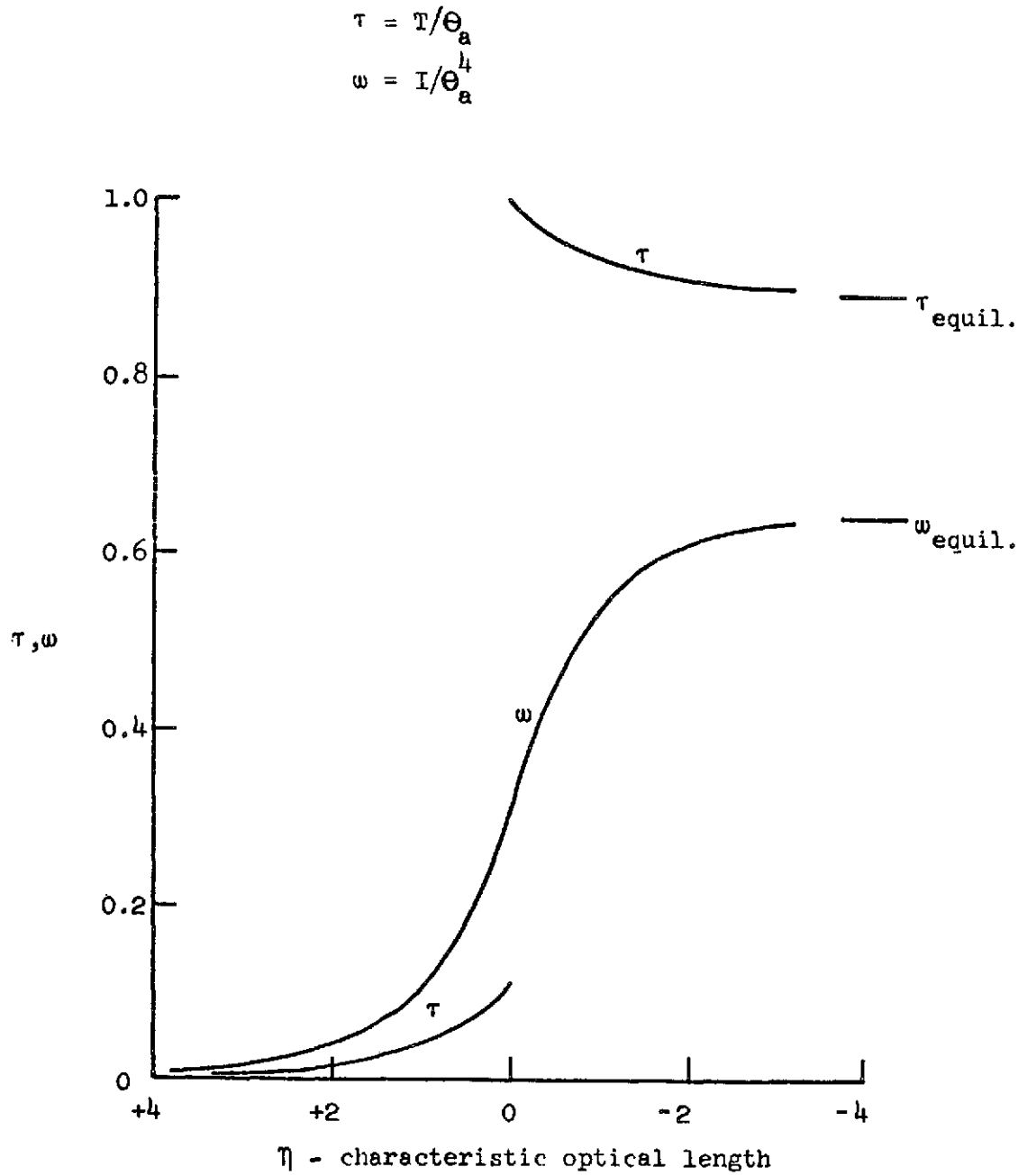

Figure 4. Numerical results of the radiation shock structure

APPENDIX

Numerical Solution of the Radiation Shock Structure for Four Values of the Boltzmann Number

The energy and transfer equations for the near-field precursor and the radiation relaxation region are solved numerically for a range of Boltzmann numbers. The equations to be solved in the near-field precursor, see equations (5.3), are:

$$-\sin\varphi \frac{\partial T_r}{\partial y_r} = \frac{4}{Bo} T_r^n (I_r - T_r^4) \quad ,$$

$$\frac{\partial}{\partial y_r}\left(\frac{1}{T_r^n}\frac{\partial I_r}{\partial y_r}\right) = 3T_r^n (I_r - T_r^4) \qquad (A.1)$$

and in the radiation relaxation region, see equations (9.3), are:

$$-\sin\varphi \frac{\partial T_a}{\partial y_a} = \frac{4}{Bo} \rho_a T_a^n (I_a - T_a^4) \quad ,$$

$$\frac{\partial}{\partial y_a}\left(\frac{1}{\rho_a T_a^n}\frac{\partial I_a}{\partial y_a}\right) = 3 \rho_a T_a^n (I_a - T_a^4 \qquad (A.2)$$

The boundary conditions for equations (A.1) are:

$$T_r \to 0 \quad , \quad I_r \to 0 \text{ as } y_r \to +\infty$$

and (A.3)

$$T_r \to \theta_r \quad , \quad I_r \to J_r \text{ as } y_r \to 0 \quad ,$$

and the boundary conditions for equations (A.2) are:

$$T_a \to \theta_B \quad , \quad I_a \to \theta_B^4 \text{ as } y_a \to -\infty$$

and (A.4)

$$T_a \to \theta_a \quad , \quad I_a \to J_r \text{ as } y_a \to 0 \quad .$$

A variable transformation of $\partial/\partial\eta_r = (1/T_r^n)\,\partial/\partial y_r$ and $\partial/\partial\eta_a = (1/\rho_a T_a^n)\,\partial/\partial y_a$, respectively, to equations (A.1) and (A.2) makes them more adaptable to numerical solution. After non-dimensionalization of the temperature by θ_B, i.e., $\tau = T/\theta_B$, and of the intensity by θ_B^4, i.e., $\omega = I/\theta_B^4$, equations (A.1) become:

$$\frac{d\omega_r}{d\tau_r} = \frac{3}{16}\,\Phi^2\,\frac{\tau_r}{(\omega_r - \tau_r^4)} \quad ,$$

$$\frac{d\eta_r}{d\tau_r} = -\frac{\Phi}{4}\,\frac{1}{(\omega_r - \tau_r^4)} \quad , \tag{A.5}$$

subject to boundary conditions:

$$\eta_r \to +\infty \quad , \quad \omega_r \to 0 \text{ as } \tau_r \to 0$$

and (A.6)

$$\eta_r \to 0 \quad , \quad \omega_r \to J_r/\theta_B^4 \text{ as } \tau_r \to \theta_r/\theta_B \quad ,$$

and equations (A.2) become:

$$\frac{d\omega_a}{d\tau_a} = \frac{3}{16}\,\Phi^2\,\frac{(\tau_a - 1)}{(\omega_a - \tau_a^4)} \quad ,$$

$$\frac{d\eta_a}{d\tau_a} = -\frac{\Phi}{4}\,\frac{1}{(\omega_a - \tau_a^4)} \quad , \tag{A.7}$$

subject to boundary condition:

$$\eta_a \to -\infty \quad , \quad \omega_a \to 1 \text{ as } \tau_a \to 1$$

and (A.8)

$$\eta_a \to 0 \quad , \quad \omega_a \to J_r/\theta_B^4 \text{ as } \tau_a \to \theta_a/\theta_B = \theta_r/\theta_B + 1 \quad ,$$

where $\Phi = Bo \sin\varphi/\theta_B^3$.

Solutions to equation (A.5) and (A.7) subject to boundary conditions (A.6) and (A.8), respectively, are given in figures 5-8 for values of Φ = 1.6, 4, 8 and 16 which correspond to values of Bo = 0.2, 0.5, 1.0 and 2.0 for $\sin\varphi = 1$.

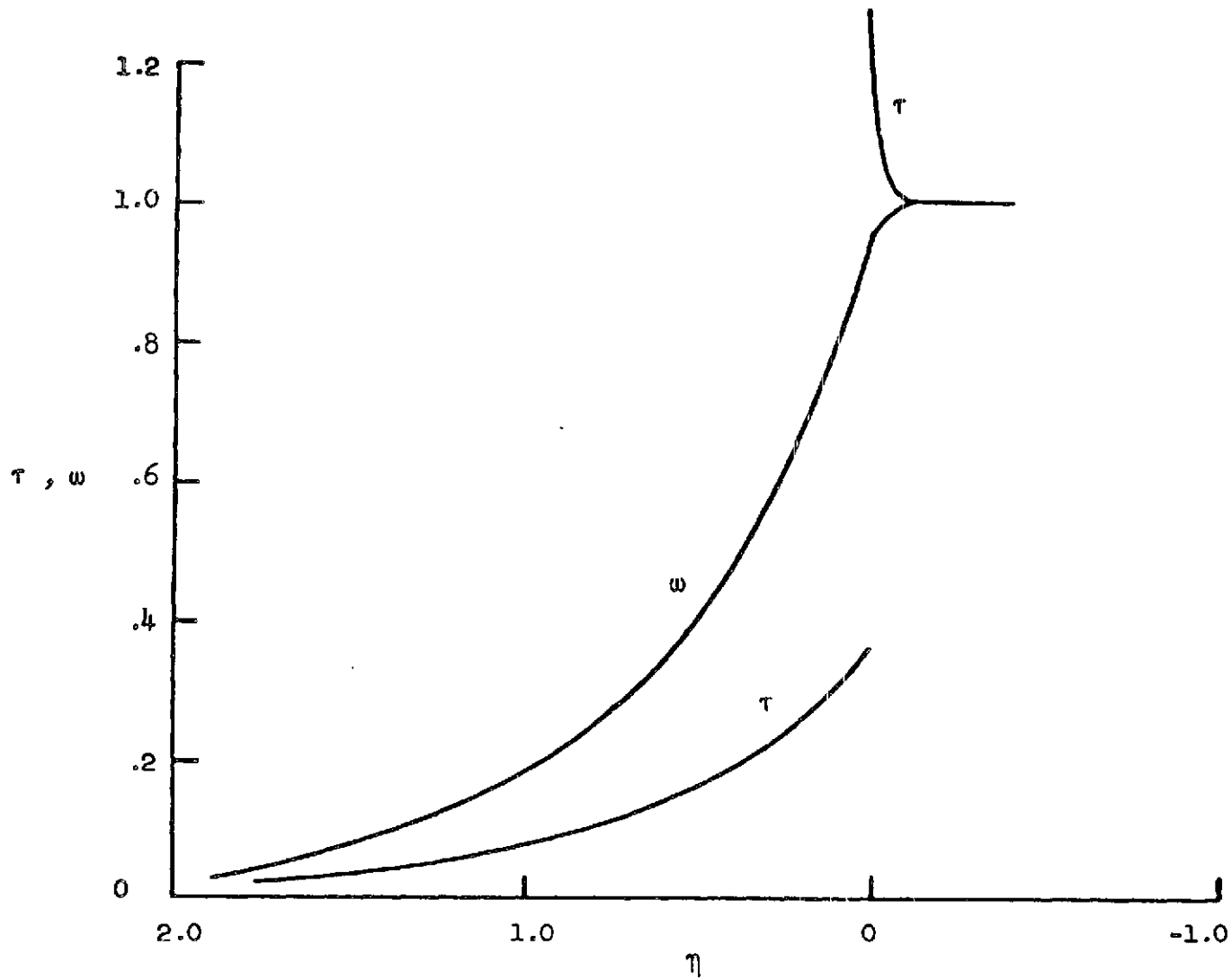

Figure 5. Radiation Shock Structure for $\Phi = 1.6$

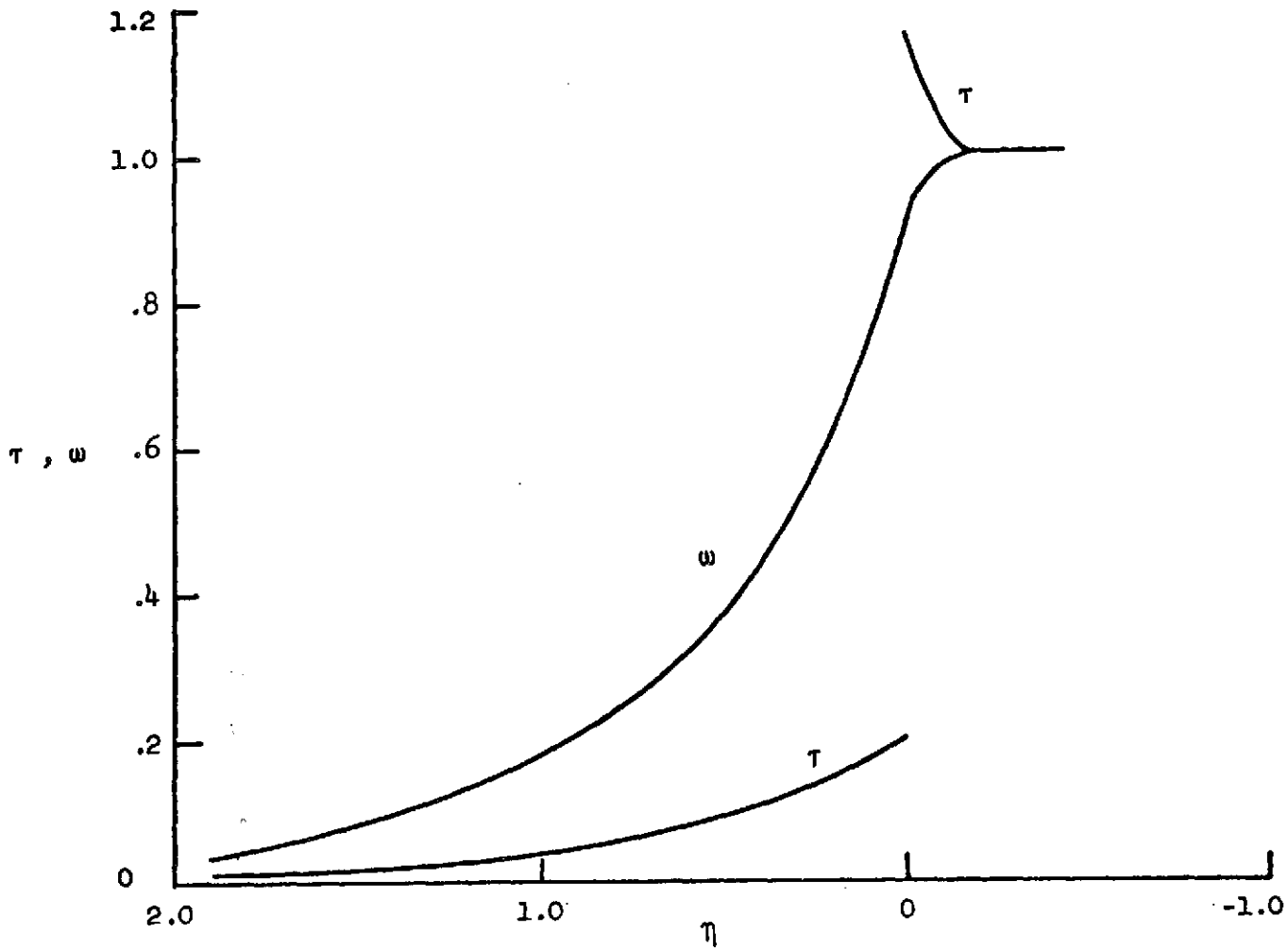

Figure 6. Radiation Shock Structure for $\phi = 4$

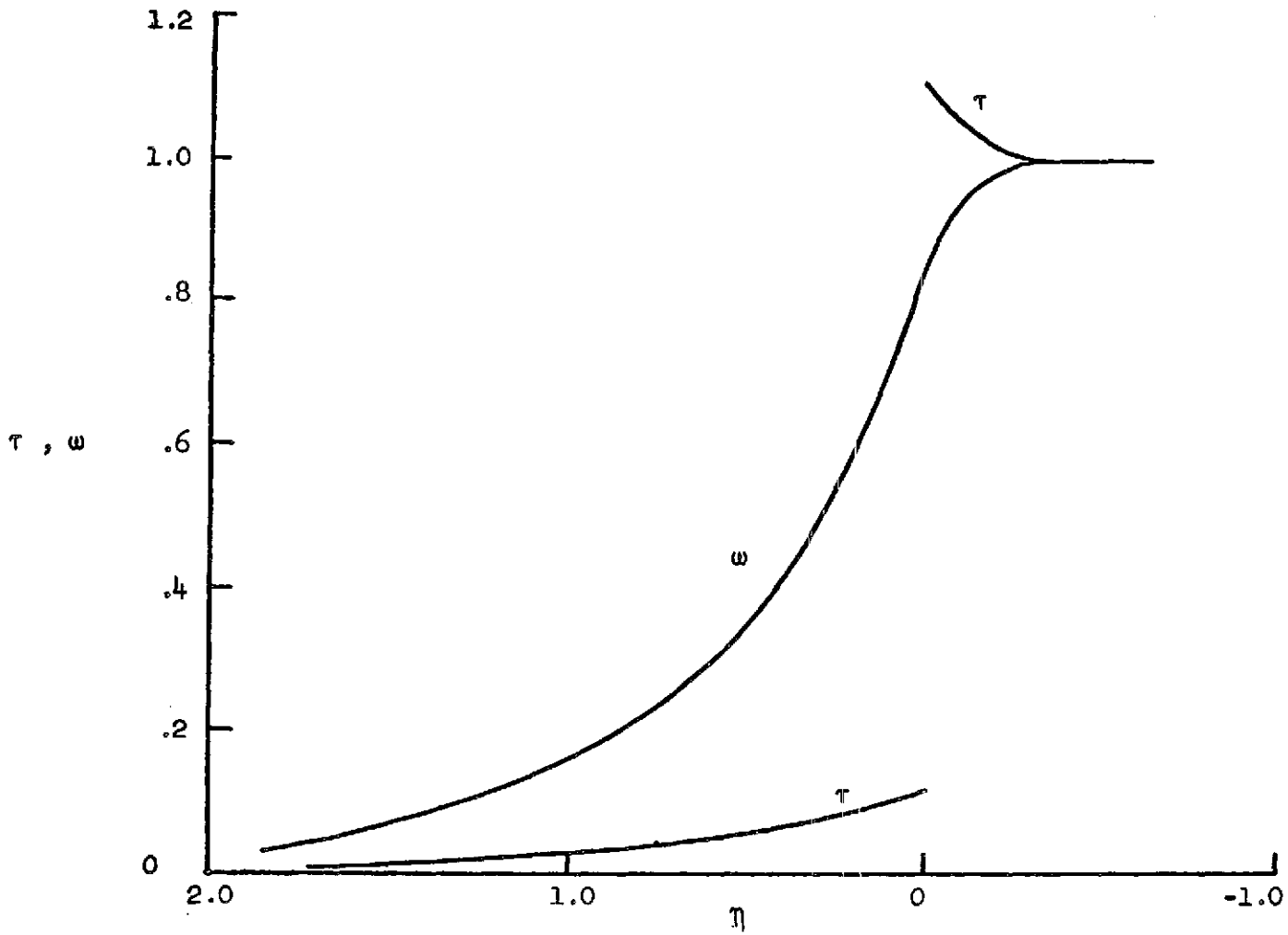

Figure 7. Radiation Shock Structure for $\Phi = 8$

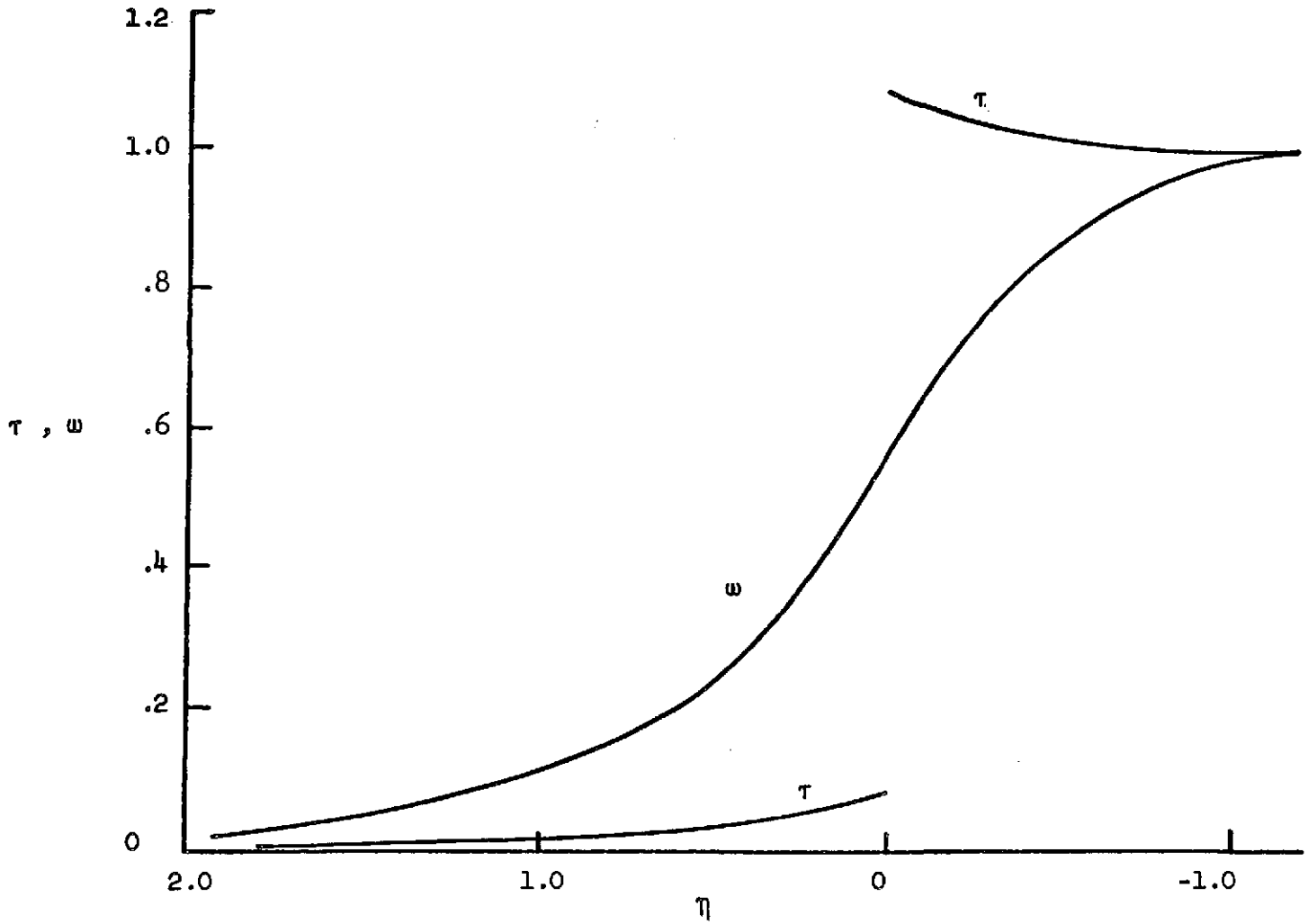

Figure 8. Radiation Shock Structure for $\Phi = 16$